DEEP SHRESTHA

ADVANCED MULTICARRIER COMMUNICATION TECHNIQUES IN AUTOMOTIVE ENVIRONMENT

Master of Science Thesis

ABSTRACT

Electronic systems in vehicles are used for advanced infotainment systems, control and automation systems, and safety critical systems. Due to increased importance of electronics in the modernization of vehicles, the size of cable harness is continuously increasing. Besides the DC wires a new cable needs to be wired for the addition of each feature in automotive environment. In addition to increased cost, the increased weight due to cabling also increases fuel consumption.

Powerline communication (PLC) exploits AC or DC powerlines without need of additional wires. Successful PLC implementation for in-vehicle environment will ease the cable burden. Using DC power supply wires as the transmission medium will enhance the vehicular efficiency. For vehicular PLC implementation, the major issue to be addressed is that the effects of interference in the vehicular environment in general, and electric cars in particular, are strong enough to seriously impair the communication link performance. Besides interference, the frequency selectivity of the transmission channel also plays a critical role. Therefore, particularly robust modulation and signal processing techniques need to be developed for this scenario.

To overcome these issues, a robust multicarrier modulation scheme is proposed in this thesis for automotive environments. The main components of this scheme include Orthogonal Frequency Division Multiplexing (OFDM) with low-order modulation and repetition coding. Furthermore, the Polynomial Cancellation Coding (PCC) method is adopted for suppressing the side-lobes in OFDM processing and effectively suppressing narrowband interferences.

PREFACE

This Master of Science thesis has been written for the completion of Master of Science (Technology) in Electrical Engineering from Tampere University of Technology, Tampere Finland. This thesis work has been carried out in Department of Electronics and Communication.

I would like to thank my supervisor Dr. Tech Markku Renfors for examining and guiding me throughout the thesis. His, support throughout the research was incredible. Thank you for always being ready to help with all the problems that I came up with.

I would like to thank my wife Sunakshi Shrestha for her continuous love and support. I would like to express my deep gratitude towards my father Mr Pawan Bhakta Shrestha, mother Mrs Raju Shrestha and brother Mr Sunny Shrestha for their continuous support throughout my study period.

Finally, thank you every one who were directly and indirectly involved for making this thesis a success for me.

Tampere, May, 2014
Deep Shrestha
deep.shrestha@student.tut.fi

TABLE OF CONTENTS

ABBREVIATIONS

1-D	One Dimension
2-D	Two Dimension
A/D	Analog to Digital Converter
BASK	Binary Amplitude Shift Keying
BPSK	Binary Phase Shift Keying
CAN	Control Area Network
CC	Cancellation Carrier
CDMA	Code Division Multiple Access
CP	Cyclic Prefix
CP-OFDM	Cyclic Prefix Orthogonal Frequency Division Multiple Access
CSMA/CA	Carrier Sense Multiple Access with Collision Avoidance
D/A	Digital to Analog Converter
DC/DC	Direct Current to Direct Current
DC-BUS	Direct Current Bus
DC-LIN	Direct Current Local Interconnect Network
DFT	Discrete Fourier Transform
DSO	Digital Storage Oscilloscope
DTFT	Discrete Time Fourier Transform
ECM	Electronic Control Module
ECU	Electronic Control Unit
FFT	Fast Fourier Transform
GI	Guard Interval
HD-PLC	High Definition Powerline Communication
HDTV	High Definition Television
IDFT	Inverse Discrete Fourier Transform
IFFT	Inverse Fast Fourier Transform
ISI	Inter Symbol Interference
LDPC	Low Density Parity Check
LIN	Local Interconnect Network
LMMSE	Linear Minimum Mean Square Error
LO	Local Oscillator
LPF	Low Pass Filter
MAC	Media Access Control
MCM	Multi Carrier Modulation
MOSFET	Metal Oxide Semiconductor Field Effect Transistor
MRC	Maximum Ratio Combining
MSE	Mean Square Error
OFDM	Orthogonal Frequency Division Multiplexing
P/S	Parallel to Serial Converter

PAM	Pulse Amplitude Modulation
PAPR	Peak to Average Power Ratio
PCC	Polynomial Cancellation Coding
PHY	Physical Layer
PLC	Powerline Communication
PSD	Power Spectral Density
PSK	Phase Shift Keying
QAM	Quadrature Amplitude Modulation
QPSK	Quadrature Phase Shift Keying
RF	Radio Frequency
RMS	Root Mean Square
RS-CC	Receiver Side Carrier Cancellation
S/P	Serial to Parallel
SER	Symbol Error Rate
S-FSK	Spread Frequency Shift Keying
SSI	Self-Symbol Interference
SW	Subcarrier Weighting
TDMA	Time Division Multiple Access
VoIP	Voice over Internet Protocol
ZP-OFDM	Zero Padded Orthogonal Frequency Division Multiplexing

1 INTRODUCTION

This chapter gives a brief introduction to the topic of the thesis. The idea of the considered technology and its main characteristics are briefly explained. Also the motivation and scope of the research is discussed. Then the research approach of this thesis work is described.

Powerline Communication (PLC) is receiving uprising interest in modern day technology. The overwhelming interest is the outcome of an inherent property that it bears. Reduction in the amount of cabling and the cost associated with it is the most attractive benefit that PLC technique imposes. PLC was used in power utilities for the first time. After 80's it has been seen to be used in home automation as well. Meanwhile, the use of PLC in automotive environment has also gained increasing interest.

The aim of PLC is to exploit power supply lines for sending and receiving information without use of external dedicated cables and wires. PLC in modern day is being utilized in many applications like power utilities for monitoring and control of faraway units, automatic remote meter reading in smart grids, Ethernet based IP-networking for home and building automation [1]. The application for home and building automation is the most potential field of PLC application due to the large number of customers available. It seems to be a very convincing way to interconnect intelligent home appliances like lights, doors and household devices, to a central home control unit. For this, a wide range of communication protocols are available, ranging from low speed and low cost X10 technology to most the recent implementation of HomePlug [2] supporting high speed communication for High Definition TV (HDTV) and Voice over Internet Protocol (VoIP).

PLC technologies can be classified with respect to the transmission frequency band and bit rate. European regulation defines the range from 3 kHz to 148.5 kHz and maximum bit rate of 1 Mbps as low frequency transmission whereas regulation for larger transmission range is ongoing. The common features of these applications are AC carrier of 50/60 Hz at medium power utilities or 110 V to 220 V for home use. In contrast to this in automotive environment powerlines operate at lower DC voltages like 3.3 V 5 V, 9 V, 12 V and 24 V complying with batteries and electronic devices requiring different coupling technology [3].

1.1   Motivation, Objective and Scope of the Research

The two key aspects that drive this research for PLC in automotive environment are:

- Physical transmission of modulated signal
- Data link and upper layers for correct communication between devices [3].

The former part is the topic of concern here in this piece of research. Study related to noises and interferences that occur due to non-linear loads (eg, motor switched on) in automotive environment are presented here as the primary focus of study. The later issue is content for flexibility and re-configurability available during application design, set up and management which is left for future work to be done further to this thesis.

Looking forward to potential automotive applications PLC technology should address solution to issues like:

- Providing better communication system, in terms of performance vs. cost, than that being used today. The requirement of adequate data rate, good responsiveness and tolerance to noise and interference should be addressed.
- Providing physical replacement to the field buses that are used today [4].

At present the main buses being used in automotive domain are: Local Interconnect Network (LIN), Control Area Network (CAN) and Flex Ray [5]. LIN provides inexpensive time trigger based communication, where reliability is not a key issue providing speed of 20 kbps with data packets of 20 bytes maximum. CAN is used for event triggered communication of messages up to 8 bytes at the speed of 1 Mbps providing a good range of versatility and reliability. In the same way Flex Ray bus is used for time-triggered communication with speed up to (2x) 10 Mbps for message up to 254 bytes. Therefore, Flex Ray bus is used for safety-critical systems and as a backbone for interconnection of different segments [3]. This thesis is mainly targeted at providing solutions for using the DC powerlines of automotive environment as a replacement for various kinds of buses like LIN, CAN and Flex Ray, for their respective purposes and use.

1.2 Research Approach

This is a simulation based research thesis. The simulation is done in MATLAB considering OFDM as robust multicarrier technique that is to be implemented. Based on various studies on the subject matter and the HPAV protocol, the feasible parameters for OFDM have been considered [6]. The PLC channel model is accounted as presented in studies done in [7]. Having a special focus on electric cars, the electric motor system introduces various types of interferences that have to be taken into account. Such interference models are taken from the studies presented in [8].

This thesis is organized in the following way: Chapter 2 explains theory and existing implementations of PLC techniques, Chapter 3 explains the basics of OFDM multicarrier scheme, as well as certain more advanced topics which were relevant for this study. Chapter 4 presents the developed robust OFDM based scheme proposed for automotive

PLC systems and defines the simulation methodology. Chapter 5 describes the simulation based performance analysis results for the proposed scheme. Chapter 6 gives the conclusions drawn from this research work, together with ideas for future work to enhance and complement this study.

2 POWERLINE COMMUNICATION

This chapter gives a brief insight to the technology called Powerline Communication (PLC). This chapter consists of three sections, namely Powerline Communication in Automotive Environment, Advantages of PLC in Automotive Environment, and in-House and in-Vehicle Powerline Communication.

PLC is a key concept that enables us to use the same cable/wire providing electrical power to devices also for the communication purpose. Power cables/wires like power grid, 240 V (low voltage cable), 20 kV (medium voltage cable), 12 V vehicle cables etc. are examples of channels that can be used as communication medium which will make all the devices connected in the network reachable without requiring additional cables/wires. Even though it is found to be beneficial to use the same cable for communication purposes, it is important to understand that powerline environment is a harsh environment due to the reasons like:

- Power distribution networks are not made for communication purpose.
- Channel is highly frequency selective in nature.
- Sources of interference are relatively high.
- Cable carrying transmission may act like radio interference to the nearby radio devices due to radiation from cable [9].

Thus, when implementing powerline communication, the above mentioned barriers should be crossed.

Due to the high reduction of cable/wire costs, implementation of PLC has a growing importance. DC-LIN (Local Interconnect Network) for vehicles, S-FSK (for meter reading, power network control and home automation), G3-PLC (for low and medium voltage network), are important standards utilizing the PLC [9]. Besides these, various research activities on implementation of PLC on vehicular environment are on-going and this is the objective of this thesis work as well.

2.1 Powerline Communication in Automotive Environment

A modern car is the amalgam of electronics and mechanical engineering where, different Electronic Control Unit (ECU) share a common power supply in the car for many onboard functions like ignition, braking, safety and infotainment systems [10]. ECUs connected with sensors and actuators are then interconnected via dedicated data lines creating a network inside car. Interaction between these ECUs provides updated view of

the system (car) as a whole and ensures quality, reliability, comfort and providing flexi-bility to the user. For the purpose of ECU interconnection different networks ranging from low data rate up to high rate namely LIN, CAN and Flex Ray have been proposed so far. Implementing these networks has significant increasing impact on the pricing of cars [6]. This is partly due to the fact that each of these networks uses network specific wires and protocols. Thus, an attractive solution to reduce the burden caused by this cable increment is PLC network utilizing DC powerline cables in automotive environ-ment.

Implementing PLC in automotive environment directly relates to the reduction in the amount of cabling, splicing of cables by simplifying the cable bundles resulting in reduced cost burden and weight of automotive vehicles. Moreover the car design must take into account the feasible cable paths to facilitate interconnection between ECUs. In vehicular applications like motorsports an expensive connector is liable to carry tens to hundreds of wires per cable. Reducing this cable bundle will have positive impact on system complexity, cost and reliability of the connectors. In the context of ECUs being used today, almost 20% of their size is used for contacts and physical connections, which implies that reduction in cables will ensure tidy sized ECUs with less production cost [11].

PLC in automotive environment presents some drawbacks along with the advanta-geous serenity. The major issue is low performance of PLC in comparison with existing Flex Ray technology [4]. This situation persists in automotive domain, apart from home and building automation, where PLC outperforms field buses used in automotive do-main in terms of available data rates. Contrary to this, the bandwidth offered by automo-tive PLC systems is comparable to other field buses used in automobiles i.e. LIN and CAN.

Even though implementing PLC for automotive vehicles provides clear cost reduc-tion due to reduced cable harness, a balance between cost reduction due to cables and increment in cost due to network interface development for PLC should also be consid-ered. In fact, there are no network interface devices or devices to implement Medium Access Control (MAC) in today's market. Thus, these technical issues should be ad-dressed when considering PLC implementation in automotive environment [5].

Another key issue to be addressed in the context of PLC implementation in automo-tive environment is network segmentation. It is a fundamental requirement to have iso-lation and interconnection between two subnets in the network that provide different function and works for different requirements. With typical field buses that are availa-ble, the mentioned isolation and interconnection can be achieved with the use of gate-ways i.e., special ECUs connected to more than one segment for filtering the traffic in between [5]. Since there is only one battery supply in a car which powers up all the components, this makes the power cable as shared medium between them. This situation is undesirable for PLC implementation since the maximum number of nodes supported by the bus in the network might be exceeded and this kind of single segment implemen-tation might cause mutual interference between segments that should be isolated. There-

fore, when dealing with PLC issues, solutions to support segmentation should be found. Using filters that can pass current and re-route the communication signals through gateways can be an approach to achieve this target [5]. Another way to achieve this can be the use of different batteries for different network segments, which in turn, will increase the cost burden in production with space limitation, weight increment and thus is a less practical approach.

When replacing the existing field busses by PLC with proper MAC, this should be enforced in a uniform pattern such that timing and order of transmission are uniformly maintained. Without uniform MAC, the applications might act differently than expected or as they have been working with the field buses.

2.2   Advantages of PLC in Automotive Environment

Considering the advantages of PLC there are many inspiring reasons to proceed with research on its implementation in automotive environment. Even though, reduction in cabling burden is the most important factor above all. Increase in the cable network inside the car makes it a complex system for fault recognition and maintenance. Even a minor issue can cause prolonged effort for rectification due to this complexity. This issue can be directly addressed by reduction is cabling burden which can be done by PLC.

Moreover, advantages of PLC in automotive environment can be listed as below:

- Decreased weight of the car.
- Increased efficiency.
- Cost reduction.
- Efficient ECUs.
- Less complex diagnostics and maintenance.

2.3   In-House and In-Vehicle PLC Scenarios

On the basis of research conducted so far, we can conclude that a high data rate and high flexibility can be obtained for in-house implementation of PLC. But, it is not possible to make the same conclusion directly to the in-vehicle PLC because of the different environment, characteristics and topology that these scenarios bear. Thus, in this section these two scenarios and the basis of PLC implementation will be explained.

2.3.1 In-House Powerline Communication

The main concept of PLC for in-house environment is to provide Ethernet-IP class network over the 230 V AC powerline channels. To this end there are various networking protocols available. In 2000, a coalition of manufacturers was able to define a new protocol named HomePlug 1.0 [12]. This process was heavily based on Orthogonal Frequency Division Multiplexing (OFDM) [13]. This implementation has the major ad-

vantage of coping with the frequency selectivity in powerline channels. Frequency selectivity is the result of multiple reflections that occur due to loads connected to power grid and by coupling to other cables placed in the same bundle. In this protocol, PLC implementation was based on 128 equally spaced carriers from 4.3 MHz to 25 MHz with differential encoding being applied. HomePlug used CSMA/CA protocol for network access whose PHY frame format is shown in the Figure 2.1below.
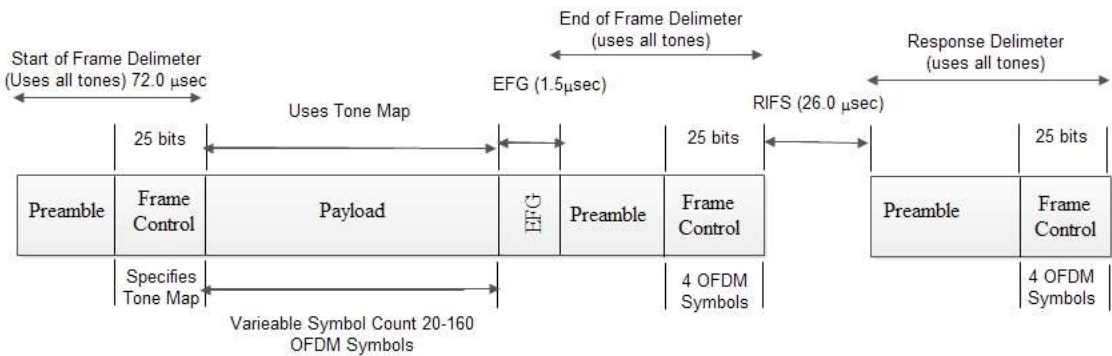

Fig 2.1. HomePlug V1.0 PHY frame format.

HomePlug AV (HPAV) was introduced as the second major standard release from HomePlug Powerline Alliance with main intention of multimedia content distribution along with data [14]. The PHY layer of HPAV operates in 2MHz to 28 MHz range providing 200 Mbps of data rate with 917 usable carriers in conjunction with flexible guard interval and independently applied modulation densities from BPSK to 1024 QPSK to each subcarrier based on channel properties. The field test results show that HPAV can achieve 10 times data rate than that of HomePlug V1.0 system [6].

Another protocol named HD-PLC proposed by Panasonic uses Wavelet OFDM achieving high efficiency in transmission with characteristics exceeding FFT-based OFDM. Wavelet OFDM forms deeper "flexible notch" preventing interference with no guard interval inserted. The MAC layer in this protocol uses hybrid TDMA and CSMA/CA protocol synchronized with AC line cycle for network access. Apart from this, Table 2.1 below shows available protocols in the market and their comparison [15].

2.3.2 In-Vehicle Powerline Communication

In-vehicle is an environment where various strong sources of interference and noise are always expected in the channel. Interferences of impulsive nature may be the outcome of various activities like turning ON/OFF of the motor, and in case of electric car, the motor control by itself, using infotainment systems, locking and unlocking of the doors and windows etc. Therefore in-vehicle environment is considered to be impulsive noise environment. The physical (PHY) layer and data link layer performances are areas to focus in [16]. Experiments to determine the properties of the automotive in board PLC supply networks have been investigated in [17] and [18]. The automotive PLC supply

network showed insertion losses of -15 dB and -36 dB over 0 MHz to 30 MHz bandwidth in the frequency range of 0.5 MHz to 30 MHz. The increasing back ground noise was found to be in 0 MHz to 100 MHz range. Especially below 10 MHz noise peaks were in the range of -90 dBm/Hz to -40 dBm/Hz. To address this situation a new cable harness structure has been proposed in [16] with star topology and star couplers where transfer function of wire is flat over the range 150 MHz to 250 MHz. However, this solution is not practical since harness structure differs from vehicle to vehicle. As varying space between cabling and car body results in changing behavior of the whole system.

PLC for PHY in 12 V powerline, as a combination of LIN protocol with PLC driver, has been proposed in [19]. In the study the interference between the master and slave nodes is avoided by adopting of different transmission modes, Binary Phase Shift Keying (BPSK) from master to slave transfers and Binary Amplitude Shift Keying (BASK) from slave to master transfers. With data rates of below 10 kbps this option is not considered to be a trust worthy solution as it cannot replace X-by-wire applications. Since,

Table 2.1. Various In-House PLC protocols proposed by various vendors.

Properties	*Panasonic*	*HPAV*	*UPA*
Modulation	Wavelet OFDM	Windowed OFDM	Windowed OFDM
Channel coding	RS-CC LDPC	Parallel-concatenated turbo convolution coding	RS + 4D-TCM concatenation
Mapping	PAM 2-32	QAM 2, 4, 6, 8, 16, 64, 256, 1024	ADPSK 2-1024
FFT/FB size	512(extendable to 2048)	3072	NC
Maximum number of carriers	NC	1536	1536
Sample frequency	62.5 MHz	75 MHz	NC
Frequency band	4-28 MHz 2-28 MHz	2-28 MHz	0-30 MHz 0-20 MHz optional
PHY Rate	190 Mbps	200 Mbps	200 Mbps
Information Rate	NC	150 Mbps	158 Mbps
Programmable notches	Yes	Yes	Yes
Power Spectral Density	NC	-56 dBm/Hz	-56 dBm/Hz
Media access method	TDMA-CSMA/CA	TDMA-CSMA/CA	ADTM
Hidden Node Avoidance	NC	Yes	Yes
Duration MAC frame	NC	Variable	Variable
Maximum number of nodes	64	NC	64
Network identifier	Yes	Yes	Yes

X-by-wire system is safety related fault tolerant system requiring precise and faster communication.

A similar approach combining CAN and PLC using DC-BUS technology with bit rate of 1.7 Mbps, narrow band channels with center frequency between 2 MHz to 12 MHz, CSMA/CA protocol supporting up to 16 nodes has been proposed as redundant channel for CAN protocol in [20], [21] and [22]. But also this solution could not answer to requirement of data rate over 10 Mbps.

Regardless of this, the study related to automotive environment concerning fuel cars and electric cars with two ECUs and two DCB500 transceivers for communication using DC wire have been done [23]. This study showed that both the environment have similar behaviors in terms of frequency channel and noise for PLC applications [24].

Considering both MAC and PHY layer communication protocol it has been shown that spread spectrum techniques like Code Division Multiple Access (CDMA) and OFDM are the candidate technologies for the implementation of PLC. OFDM outperforms CDMA in context of high data rate and throughput while encountering frequency selectivity of the powerline channel [25].

To overcome the present ambiguous situation a single robust technology that is able to encounter the interferences in the channel and overcomes the frequency selectivity is a critical required for PLC implementation in automotive environment.

3 PRICIPLES OF OFDM

This chapter lays out the fundamental background of OFDM. This chapter is further divided into three sections. The first section explains the basic OFDM model defining the foundations of OFDM based on orthogonality and IFFT/FFT implementation with the use of Cyclic Prefix (CP) and explains pros and cons of this technique. In the same manner, the second section deals with the OFDM spectrum and its estimation. At last the third section describes side lobe suppression techniques like Polynomial Cancellation Coding, Time Domain Windowing, Cancellation Carriers and Subcarrier Weighting that are needed for efficient OFDM operation in the presence of narrowband interferences.

3.1 Fundamentals of OFDM

OFDM is a Multi Carrier Modulation (MCM) scheme where high rate serial data stream is converted to low rate parallel data streams and is transmitted over channel whose bandwidth is divided into orthogonal subcarriers. Each symbol from the parallel data stream is then modulated with different sub carrier on different frequency simultaneously [26].Thus, regardless of conventional transmission system where the whole symbol block occupies the whole bandwidth, in OFDM each data symbol is found to utilize a portion of the bandwidth. The use of orthogonality between subcarriers yields high spectral efficiency and hence is the main advantage of OFDM technique, which is illustrated in Figure 3.1 below.
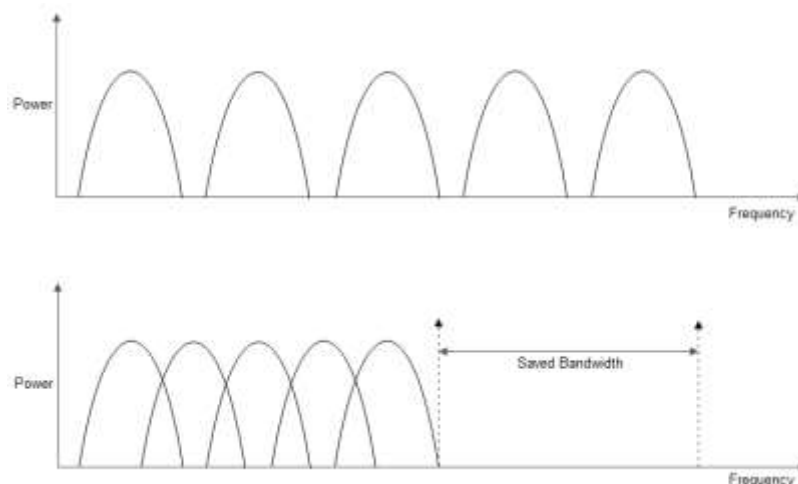

Figure 3.1. a) Conventional multicarrier signal spectrum b) OFDM spectrum.

Orthogonality in OFDM is achieved through implementation by Inverse Fast Fourier Transform (IFFT) in the transmitting end and Fast Fourier Transform (FFT) block at the receiving end. Apart from this implementation of IFFT and FFT block further helps in simplifying the channel equalization process with reduced computational complexity. Through the easy equalization process OFDM overcomes the Inter Symbol Interference (ISI) and multipath effects. These effects can be encountered by the use of cyclic prefix (CP), which is the replica of the end part of the transmitted data block [27].

OFDM can also encounter the frequency selectivity in the communication channel. In case of a wideband communication channel, narrow-band frequency selective fades only a few subcarriers in OFDM, unlike the conventional single carrier schemes where one signal fade can destroy large amount of data. With implementation of effective error correction schemes it is possible to reach reliable link performance with severely frequency selective channels [28].

OFDM Model

OFDM modulates symbols to different subcarriers which are orthogonal to each other. OFDM uses subcarriers of the form $\phi(t) = exp[j2\pi fkt]$. In OFDM modulating, a set of N complex random, independent and identically distributed symbols $\{x_0, x_1,.., x_{N-1}\}$ are modulated to N subcarriers. The subcarrier is represented in equation (3.1)

$$y(t) = \exp[j2\pi f_k t].$$
(3.1)

The modulated OFDM symbol can then be expressed as:

$$y(t) = \sum_{k=0}^{N-1} x_k \exp[j2\pi f_k t].$$
(3.2)

Hence, the modulated OFDM symbol is a sum of N frequency shifted subcarriers weighted by data samples x_k as shown in Figure 3.2. To maintain orthogonality between subcarriers it is essential to define a suitable frequency shift. Mathematically, orthogonality is defined as zero correlation between two functions within same interval [29]. Therefore, the use of orthogonality characteristic eliminates the interference that might occur between consecutive subcarriers and hence no guard band is required between them. To achieve orthogonality, the following condition needs to be satisfied:

$$\langle f_m, f_n \rangle = \int_a^b f_m^*(x) f_n(x) dx = 0 \; if \; m \neq n. \tag{3.3}$$

On attempt to full fill the orthogonality condition in OFDM:

$$\langle y_k, y_l \rangle = \int_0^{T_u} y_k^*(t) y_l(t) dt$$

$$= \int_0^{T_u} x_k^* \exp[-j2\pi f_k t] x_l \exp[j2\pi f_l t] dt$$

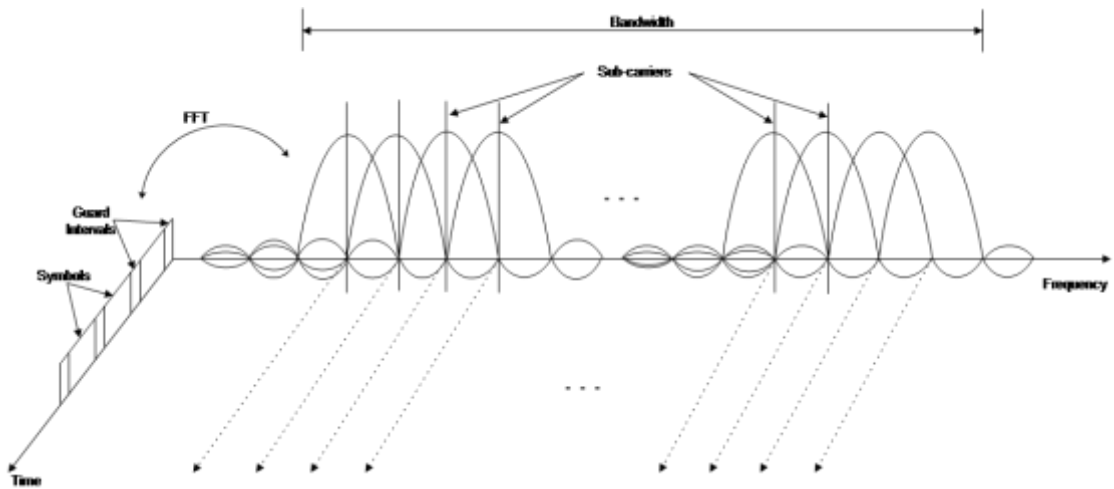$$= x_k^* x_l \frac{\exp[j2\pi T_u(f_l - f_k)] - 1}{j2\pi(f_l - f_k)} \tag{3.4}$$

Figure 3.2. OFDM signal.

From equation (3.4) it is seen that if $2\pi T_u(f_l - f_k) = 2m\pi$, where m is an integer, then value of $\langle y_k, y_l \rangle$ becomes 0. As a conclusion it can be drawn that orthogonality between OFDM subcarriers are maintained when:

$$f_l - f_k = \frac{m}{T_u}. \tag{3.5}$$

Thus, subcarrier spacing of $1/T_u$ is the smallest possible frequency spacing which gives orthogonality and thus results in highest spectral efficiency in OFDM. Therefore substituting $f_k = k/T_u$ in equation (3.2), the expression of OFDM symbol becomes:

$$y(t) = \sum_{k=0}^{N-1} x_k \exp\left[j2\pi t \frac{k}{T_u}\right].$$ (3.6)

In discrete-time model, the OFDM symbols can be expressed as:

(3.7)
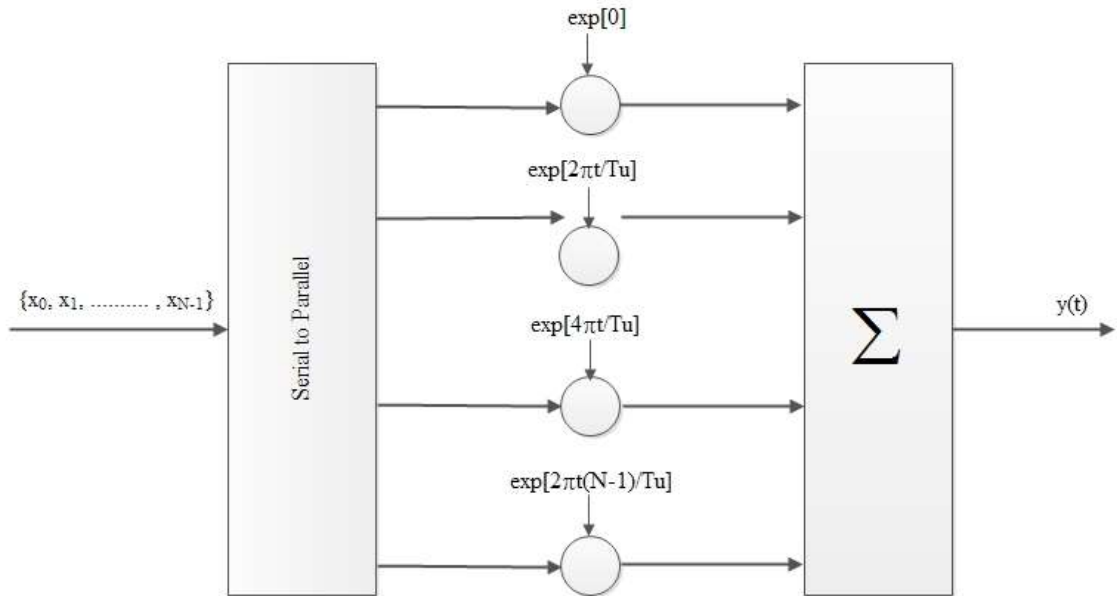$$y(nT) = \sum_{k=0}^{N-1} x_k \exp\left[j2\pi n \frac{k}{N}\right]$$

Figure 3.3. Basic OFDM implementation block.

A simple implementation of OFDM symbol generation is shown in Figure 3.3. It consists of a serial-to-parallel (S/P) converter after which the symbols are modulated with subcarriers at multiples of $1/T_u$ interval and finally being summed up to from an OFDM symbol.

3.1.1 Implementation of IFFT/FFT in OFDM

OFDM can be implemented efficiently using IFFT algorithm for Inverse Discrete Fourier Transform (IDFT) and FFT algorithm for Discrete Fourier Transform (DFT) calculations as:

$$y_n = \sum_{k=0}^{N_{FFT}-1} X_k \exp[j2\pi kn/N_{FFT}] . \qquad (3.8)$$

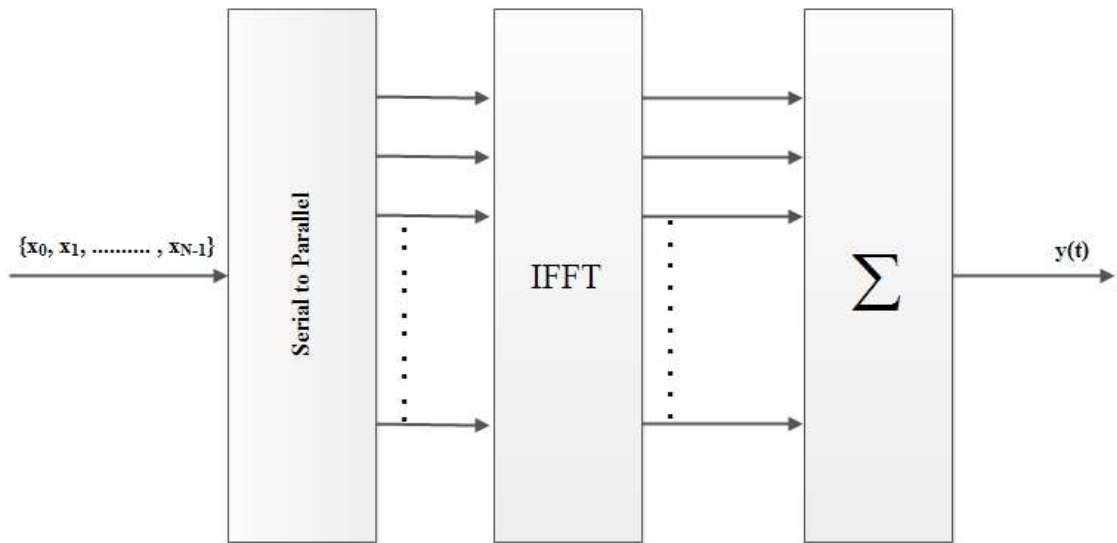$$X_k = \sum_{k=0}^{N_{FFT}-1} y_n \exp[-j2\pi kn/N_{FFT}] \qquad (3.9)$$

Figure 3.4. Implementation of IFFT in OFDM.

Here equation (3.8) denotes IDFT and equation (3.9) represents DFT operation [30] with transform length of N_{FFT}. Implementation of IFFT/FFT in OFDM is shown in Figure 3.4 where computational effort is highly reduced. Use of IDFT block as modulator corresponds operations proportional to $O(N^2)$, whereas the calculation complexity is reduced by $O(N \log N)$ operations with effective implementation of IFFT/FFT block in OFDM.

3.1.2 Cyclic Prefix/Guard Interval

Multipath propagation results from summation of delayed version of symbols being transmitted due to reflections and diffractions. Multipath propagation causes overlap of consecutive symbols resulting in Inter Symbol Interference (ISI) and destroying the perfect orthogonality between sub-channels in a practical OFDM. The addition of Inter Carrier Interference (ICI) and Inter symbol Interference (ISI) from the transmission channel itself makes the separation of sub-carriers with FFT implementation difficult at

the OFDM receiver. In the presence of multipath propagation in transmission channel the receiver actually receives multiple copies of the original signal at the same time. Thus, to overcome the consequences of ISI, a guard interval (Δ_g) is added to every OFDM symbols [28].

Delay spread is the longest delay that a multipath component may have due to the transmission channel. So, a guard interval (Δ_g) longer than the channel delay spread should be used to overcome the effect of ISI. After inserting the guard intervals, the total symbol duration (T_s) of OFDM symbol will be the sum of the useful symbol duration (T_u) and guard interval (Δ_g)

$$T_s = T_u + \Delta_g \tag{3.10}$$

However, Self-Symbol Interference (SSI) resulting from interference between samples of same OFDM symbol is not eliminated by use of guard interval which rather should be equalized in the receiver.

Another effect to overcome in OFDM is the ICI occurring due to the lack of orthogonality between two sub carriers. To overcome these effects the concept of using cyclically extended OFDM symbols is commonly used. Copying a guard interval duration of symbol from end and placing it the front of each symbol accomplishes this idea, which is called as Cyclic Prefix (CP).
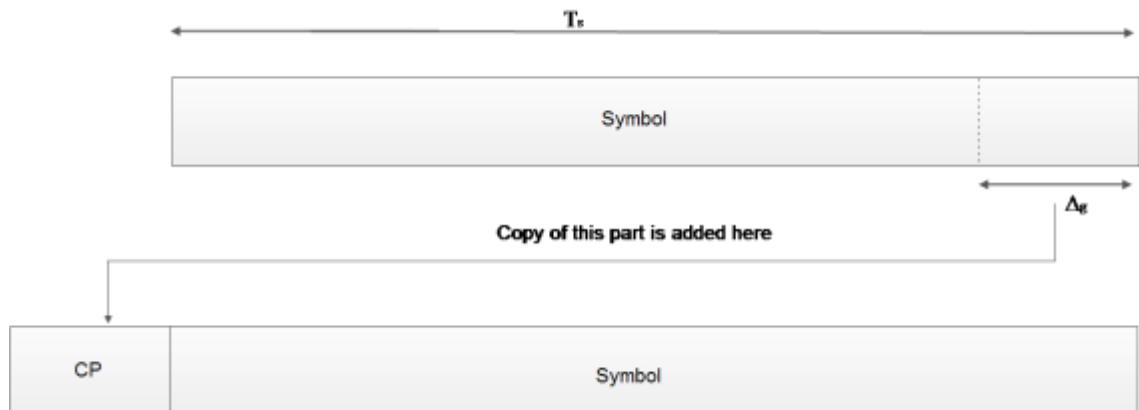

Figure 3.5. Cyclic prefix and Guard Interval in multipath channel.

Figure 3.5 above shows an OFDM symbol and its delayed version after insertion of the cyclic prefix. The periodicity of the CP is further utilized for symbol synchronization at the receiver end and also for estimation of the delay.

OFDM Implementation

A basic system level block diagram of an OFDM transmission link is shown in Figure 3.6. The transmitter side comprises of Serial to Parallel (S/P) convertor with encoder, mapper, IFFT block, guard interval (GI) addition block, Parallel to Serial (P/S) conver-

tor, Digital to Analog (D/A) convertor, Low Pass Filter (LPF) and RF Modulator in sequence. The receiver side comprises of Radio Frequency (RF) Demodulator, LPF block, Analog to Digital (A/D) convertor, S/P block, guard band removal block, FFT block, Equalizer/Estimation block, De-mapper block, and P/S with Decoder.
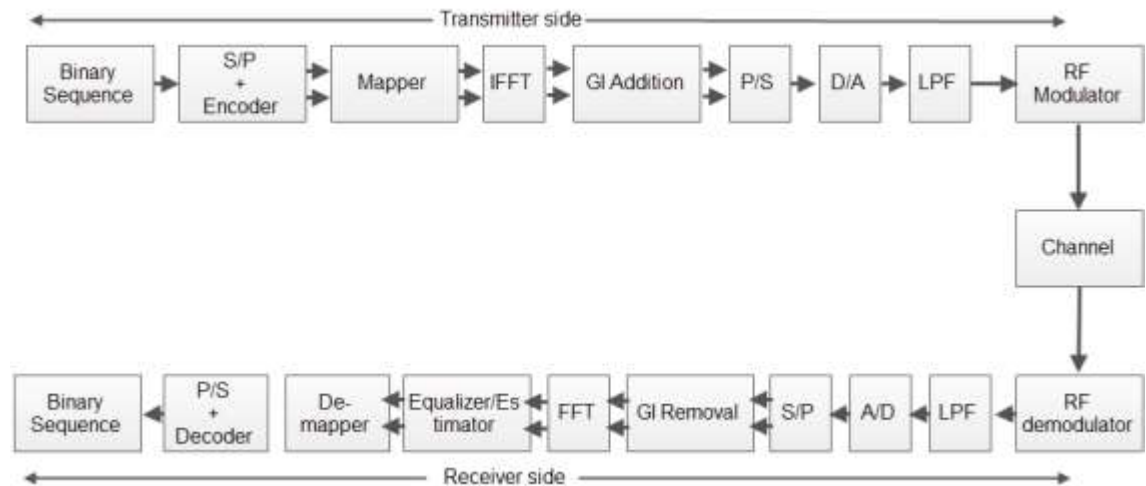

Figure 3.6. Basic OFDM system model.

On the transmitting side, the first thing to be done is conversion of a serial binary bit stream of data into a parallel bit streams. These parallel bits of data are then grouped based on applied modulation technique producing complex symbol sequences by the mapper block. These symbols are then modulated in baseband by IFFT, after which the addition of GI is done to each OFDM symbols. After this, the parallel set of samples are then converted back to serial form in the P/S block. The data is so far processed in digital form, which cannot be transmitted through physical channel. Therefore, the data samples need to be converted into analog form by D/A converter and LPF blocks. Furthermore, the produced continuous-time baseband signal is shifted to pass band by the RF modulator making the signal ready for transmission through channel. During the transmission, the properties of the channel and the transmission environment makes modifications in the transmitted signal which should be combated at the receiver end for error free communication between the transmitter and receiver.

At the receiver end almost all the operations done on the transmitting side are performed in reverse order with some additional blocks performing some additional functions that are not required while transmitting. The equalizer/estimator block at the receiver side removes unwanted signal attenuation effect that transmission channel and environment has on the symbols being transmitted. The decoder at receiver called as soft decoder works to decode received symbols back to original form. The decoding process is based on decisions made on reliability ground of the received symbols. Thus, finally a transmitted sequence of data is reproduced at the receiver end.

3.1.3   Pros and Cons of OFDM

There are many distinctive features making OFDM a superior choice over conventional single carrier transmission system. The spectral overlapping of subcarriers in OFDM provides spectral efficiency which is achieved in a computationally effective way with the use of IFFT/FFT blocks preserving orthogonality between subcarriers. The spectral fragmentation used in OFDM provides simple channel equalization scheme providing robustness against multipath fading and eliminating ISI. As a result guard band is not required between subcarriers in OFDM which saves valuable frequency resource. Apart from spectral efficiency, OFDM has transmission flexibility with adaptability. Therefore, various modulation and coding techniques can be used between subcarriers according to the transmission quality requirements of each user.

Arising from non-ideal OFDM implementation and impacts of the communication channel on OFDM signals, OFDM bears also various drawbacks. In the OFDM spectrum, side-lobes are found around the useful part of OFDM spectrum, i.e., outside the frequency range of the active subcarriers. These side-lobes bear relatively high power which introduces interference to the signals transmitted in adjacent frequency channels, which are not precisely synchronized in time and frequency to the OFDM symbol sequence. On the receiver side, the basic OFDM processing is not able to suppress the adjacent channel signals effectively, unless they are precisely synchronized to the received OFDM signal. To reduce this effect of interference guard bands are inserted around active OFDM subcarriers to suppress the side-lobes from the neighbouring channels. This implementation in turn reduces spectral efficiency.

Another major drawback with the OFDM system is high peak-to-average power ratio (PAPR). High PAPR is the result of multicarrier modulation. An OFDM symbol is the sum of all sample values multiplied by complex exponentials which are sum of real cosine and imaginary sine waves, as shown in equation (3.6). At some point of time these cosines and sines sum up in magnitude to produce a much higher peak than RMS value of the OFDM symbol. This high PAPR is disadvantageous to OFDM system because it requires high linearity in the amplifiers of the transmission chain because non-linear amplifier gets saturated with the high peaks and produces unfavourable inter modulation products to the OFDM spectrum. The effect is particularly critical for the transmitter power amplifier. Thus, to reduce the problem of high PAPR techniques like Tone Reservation, Tone Injection and Partial Transmit Sequence can be used [31].

The sensitivities towards frequency and timing offsets resulting due to the practical transmitter and receiver non-ideality are the other major drawbacks and challenge that the OFDM systems have. To eliminate these two major drawbacks an accurate synchronization at the receiver end is needed. Timing synchronization enables detection of the beginning of ISI free part of each received OFDM. When the CP is longer than the channel delay spread, the periodicity of the CP-OFDM can be used for estimating the timing error. Too short CP causes loss of orthogonality between subcarriers and degrades the link performance by increasing the Bit Error Rate (BER). Two approaches

based on pilot symbols and cyclic prefix structures are used for timing offset estimation [27]. The difference in the carrier frequency and receiver Local Oscillator (LO) frequency creates frequency offset error. The offset frequency is the result of the inaccuracies of the LO's and Doppler Shift due to transmitter and receiver movement. Frequency offset destroys the orthogonality of subcarriers making received subcarrier signals affected by neighbouring subcarrier, thus causing ICI.

3.2   Power Spectral Density and its Estimation

Power of a signal is defined as the average energy that the signal holds over time. Power spectral density (PSD) defines distribution of power with respect to frequency. Therefore, PSD can further be elaborated as average energy of spectral density of time period where $T \rightarrow \infty$ at ω. Energy spectral density is the mean squared value of signal in frequency domain indicated by $X(\omega)$. Mathematical definition of energy spectral density and PSD can be expressed as follows:

$$S_{xx}(\omega, T) = E[|X(\omega, T)|^2]\tag{3.11}$$

$$P_{xx}(\omega) = \lim_{T \rightarrow \infty} \frac{S_{xx}(\omega, T)}{T} = \lim_{T \rightarrow \infty} \frac{E[|X(\omega, T)|^2]}{T}\tag{3.12}$$

The above equations can be implemented discrete time signals by replacing time period T with number of samples in the observation [32]. In practice, OFDM is implemented using discrete-time signal processing scheme. Due, to this DFT and DTFT can be used to evaluate the spectrum. DTFT represents signal x_n in terms of exponential sequence of continuous frequency expressed as exp[-j ωn]. The mathematical representation of this concept is as follows:

$$Y(e^{j\omega}) = \sum_{n=-\infty}^{\infty} x_n exp[-j\omega n]\tag{3.13}$$

The result is always a periodic continuous function of period 2π. Now, DFT can be obtained using DTFT results sampled at N_{FFT} equally spaced points [30].

A finite length signal can be multiplied by rectangular window of T_u and unity amplitude. Therefore, the spectrum of any time-limited signal is the convolution of an unlimited signal spectrum and a rectangular window. DFT considers frequency representation of periodic time signal with N periods. It means that DFT treats limited sequence in time domain as infinitely repeated sequence. If the window length is not equal to signal

period or it's multiple then resulting spectrum contains some leakage effects [33]. A perfect periodicity in signal defines DFT bin location at the same position of signal frequency component in frequency axis. This is a rare case to happen. Most often the frequency bins are not located at signal frequency components because of the discontinuity between signal ends. The result is that the frequency bins contain energy that is leaked from neighbouring frequency components. Thus, to reduce the effect of energy leakage, the number of DFT points should be increased improving frequency resolution.

After the serial-to-parallel block in the OFDM transmitter, a set of parallel phase shift keying (PSK) or quadrature amplitude modulation (QAM) symbols are fed to IFFT block. Thus, it is required to have a careful examination of the OFDM implementation specifics. An OFDM symbol multiplied by time-shifted rectangular window can be expressed in time and frequency domains as:

$$y(t) = \sum_{c=0}^{\infty} \left[\sum_{k=0}^{N-1} x_{k,c} exp[j2\pi k(t - cT_u)/T_u] \right] rect \left[\frac{t - cT_u}{T_u} \right]. \tag{3.14}$$

$$y(f) = T_u \sum_{c=0}^{\infty} exp[j2\pi fT_u c] \sum_{k=0}^{N-1} x_{k,c} sinc[fT_u - k] \tag{3.15}$$

Thus, the resulting PSD is given by equation (3.16).

$$P_y(f) = T_u \sum_{k=0}^{N-1} E \left[|x_{k,c}|^2 \right] |sinc[fT_u - k]|^2 \tag{3.16}$$

Here, equations (3.15) and (3.16) are the weighted sinc functions where each subcarriers are represented by a shifted sinc. Due to the presence of sinc function there are ripples around the centre. These ripples of each subcarrier get engaged with each other creating interference between them. Therefore, orthogonality between the subcarriers in OFDM should be maintained. By maintaining a healthy orthogonality between the subcarriers makes these ripples to intersect frequency axis at centre frequencies of other subcarriers. This results in no interference in the useful range. Subcarrier ripples that are accumulated outside of the useful band are generally creating high power ripples. Thus, there is reduction in spectral efficiency due to OFDM side-lobes. Hence, side lobe reduction techniques are required for better efficiency.

Cyclic prefix also has some spectral effect in OFDM. CP extends the rectangular function duration from T_u to T_s. Equation (3.14) is now updated as follows:

$$y(t) = \sum_{c=0}^{\infty} \left[\sum_{k=-N_{CP}}^{N-1} x_{mod(k,N-1),c} exp[j2\pi mod(k, N-1)(t - cT_s)/T_u] \right] rect \left[\frac{t - cT_s}{T_s} \right]$$

$$(3.17)$$

Since, the data samples in CP are copied data, therefore their frequency components are contained in the interval $[0, k]$. Thus, OFDM spectrum should now be evaluated as:

$$Y(f) = \sum_{c=0}^{\infty} T_s exp[j2\pi f T_s c] \left[\sum_{k=0}^{N-1} x_{k,c} \delta \left[f - \frac{k}{T_u} \right] \right] * sinc[f T_s]$$

$$(3.18)$$

$$= T_s \sum_{c=0}^{\infty} exp[j2\pi f T_s c] \sum_{k=0}^{N-1} x_{k,c} sinc \left[T_s \left(f - \frac{k}{T_u} \right) \right]$$

With $x_{k,c}$ as i.i.d symbol sequence, the PSD is given as [34]:

$$P_y(f) = T_s \sum_{c=0}^{\infty} \sum_{k=0}^{N-1} E\left[|x_{k,c}|^2 \right] \left| sinc \left[T_s \left(f - \frac{k}{T_u} \right) \right] \right|^2 \qquad (3.19)$$

As a result of the CP effect, zero intersections of sinc function are changed. As seen in the equation (3.15) and (3.16) the sinc function intersects zero at frequencies corresponding to $\frac{i+k}{T_u}$, where k is index of subcarrier and i is positive integer. Here, subcarriers do not overlap whereas in equations (3.17) and (3.18) sinc function zero intersections are in frequencies of $\frac{i}{T_s} + \frac{i}{T_u}$. This causes overlapping of subcarriers at centre frequency of $\frac{1}{T_u}$ resulting in loss of orthogonality. But, this effect can be removed at the receiver side through the CP removal.

Zero-Padding OFDM (ZP-OFDM) is considered as another alternative where guard interval is filled with zeroes instead of data samples. In ZP-OFDM, the signal is multiplied with a rectangle of length T_u. As a result, the spectrum becomes similar to that of OFDM without any CP. Thus, equations (3.15) and (3.16) are valid for ZP-OFDM with normalization factor of T_u is replaced by T_s to consider time extension.

3.3   OFDM Side Lobe Suppression

The side-lobes with high power normally limit the spectral usage around active subcarriers. To supress the high powered side-lobes, additional techniques need to be imple-

mented. Techniques like polynomial cancellation coding, time domain windowing, cancellation carriers and subcarrier weighting have been proposed by many studies and research being done so far [35].

3.3.1 Polynomial Cancellation Coding (PCC)

Polynomial cancellation coding (PCC) reduces frequency sensitivity and phase error in OFDM [36]. PCC reduces side lobe power significantly. PCC divides useful part of IFFT block into identical groups. Each group containing *m* subcarriers represents one data symbol in a way where each subcarrier in the group is multiplied by coefficients of following polynomial:

$$(1 - x)^{m-1} \tag{3.20}$$

In common practice a group of two subcarriers is used in PCC. This makes the coefficient as expressed in equation (3.20) as $a_0 = 1$ and $a_1 = -1$. Thus, subcarriers in frequency domain is expressed as:

$$Y_{kP+p}(f) = T_u a_p sinc[fT_u - k - p] \text{ for } p = 0,1 \ldots P - 1 \tag{3.21}$$

In this case the spectrum is given by:

$$Y_{2k}(f) - Y_{2k+1}(f) = x_k \frac{T_u sinc[T_u f - 2k]}{T_u f - 2k - 1} \tag{3.22}$$

The resulting fraction in the above equation in fact reduces the side-lobes of OFDM spectrum [37]. There is no additional complexity in implementation of PCC, but it bears the major drawback that the spectral efficiency is reduced by the factor of two.

The resulting suppression performance of PCC is high for subcarriers that are situated far from the used subcarriers. A block diagram of PCC implementation is shown in Figure 3.7.

3.3.2 Time Domain Windowing

The rectangular shape of OFDM symbol in time domain is the main reason for high side-lobes in OFDM. This shape produces a sum of sinc functions in frequency domain. The sum of sinc side lobe results in high powered side-lobes resulting in the problems
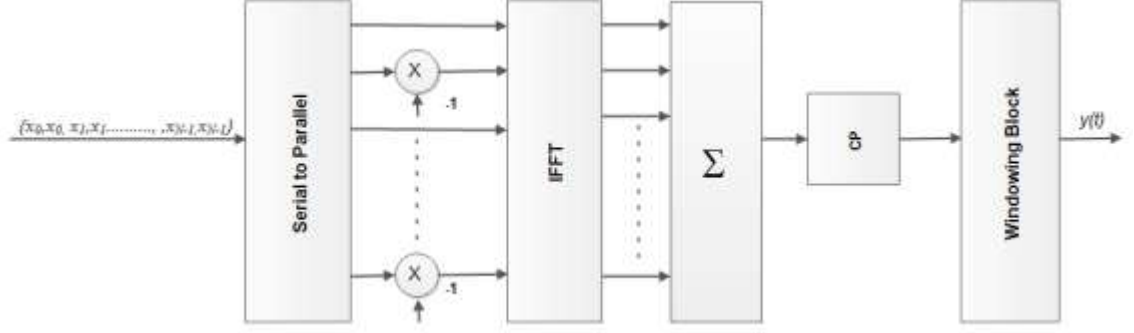
Figure 3.7. PCC-OFDM with two subcarriers in a group.

discussed earlier. The time domain windowing technique reduces the side lobe power by changing the OFDM symbol shape. This modification makes the symbol transition longer and smooth by adding slope to the symbol. Addition of such transition is done by multiplication of extended OFDM symbol in time domain with appropriate window shape that provides smoothness [38]. The addition of longer transition makes it beneficial by reducing spectral power leakage of OFDM scheme.

The size of the window that is to be used for smoothing of OFDM symbol must be based on following conditions:

- Transition length of window must be chosen based on available time resources.
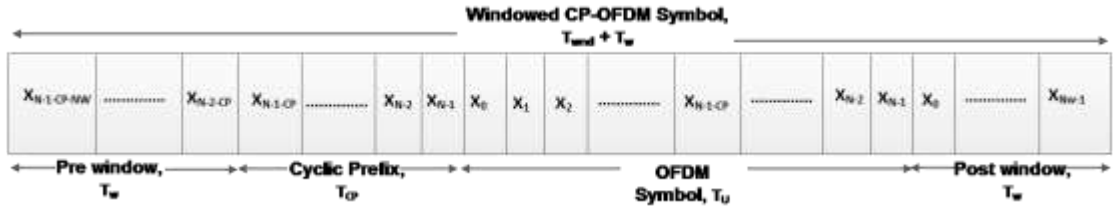- Window should not modify the symbol value.

Figure 3.8. Windowed CP-OFDM symbol structure in time domain

Thus, to achieve this block of data symbols needs to be added to the beginning (pre-window) and to the end (post-window) of OFDM symbol as shown in Figure 3.8. The time overhead caused by longer transition between symbols is reduced by allowing two consecutive OFDM symbols to interfere during pre and post-window period as shown in Figure 3.9. This window period is defined as window period of length N_w samples or T_w seconds such that overall symbol duration becomes $N_{wnd} = N_u + N_{CP} + N_w$ or $T_w = T_s + T_w$. Windowing also modifies the OFDM PSD. The PSD of windowed OFDM is expressed as:

$$P_y(f) = \sum_{k=0}^{N-1} E\left[\left|x_{k,c}\right|^2\right] \left|W(f - \frac{k}{T_u})\right|^2 \qquad (3.23)$$

Here $W(f)$ is the frequency domain representation of window $W(t)$ having time duration of $T_{wnd} + T_w$.

The Raised Cosine (RC) window is the most suitable windowing shape as it provides controllable smoothness to windowed OFDM symbol without changing symbol data or CP in time domain. The mathematical expression expressing RC window is as follows:

$$w_{RC}(t) = \begin{cases} \dfrac{1}{2} + \dfrac{1}{2} cos\left(\pi + \dfrac{\pi t}{\alpha T_{wnd}}\right) & \text{for } 0 \le t < \alpha T_{wnd} \\ 1 & \text{for } \alpha T_{wnd} \le t \le T_{wnd} \\ \dfrac{1}{2} + \dfrac{1}{2} cos\left(\dfrac{\pi(t - T_{wnd})}{\alpha T_{wnd}}\right) & \text{for } T_{wnd} \le t < (1 + \alpha)T_{wnd} \end{cases} \quad (3.24)$$

Here, α denotes the roll-off factor that controls length of window interval with $T_w = \alpha T_{wnd}$ [38]. The frequency domain representation for RC window can be expressed as in equation (3.25).

$$(3.25)$$
$$W_{RC}(f) = T_s sinc(fT_s) \left[\frac{\cos(\pi \alpha T_{wnd} f}{1 - 4\pi^2 T_{wnd}^2 f^2}\right]$$

RC window in frequency domain is a sinc function multiplied by factor $\frac{cos(\pi \alpha T_{wnd} f)}{1 - 4\pi^2 T_{wnd}^2 f^2}$ which in turn reduces the side lobe in OFDM. Figure 3.10 depicts the simple implementation model of CP-OFDM. In this implementation, the CP is extended to include also the windowed transition. An additional window block is added for multiplying each data symbol in window interval with the RC coefficients. A detailed structure of windowing block is shown in Figure 3.11 where post window of previous CP-OFDM is stored and summed with pre window of current CP-OFDM resulting in required interference window interval. Here, post window of current CP-OFDM symbol is just stored to repeat the procedure with next CP-OFDM symbol. Time domain windowing with above implementation bears some additional computational complexity as well. Thus, the added complexity can be defined as:

$$\begin{aligned} C &= 2N_w \\ A &= N_w \end{aligned} \quad (3.26)$$

where, C denotes number of real multiplication operations per OFDM symbol and A defines number of real addition/subtraction operations per OFDM symbol to be done. The computational complexity bared by time domain windowing tends to increase line-
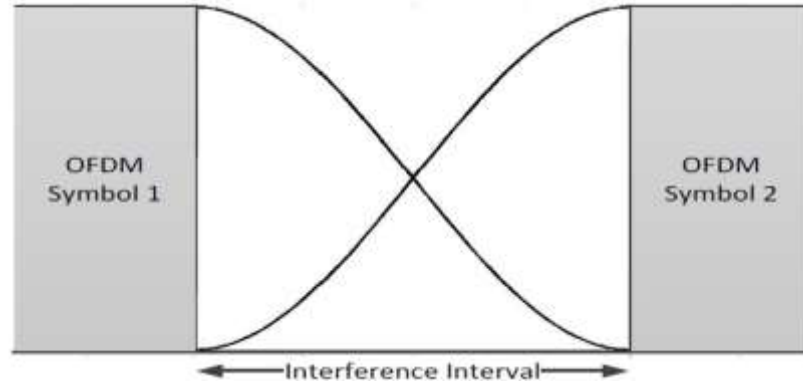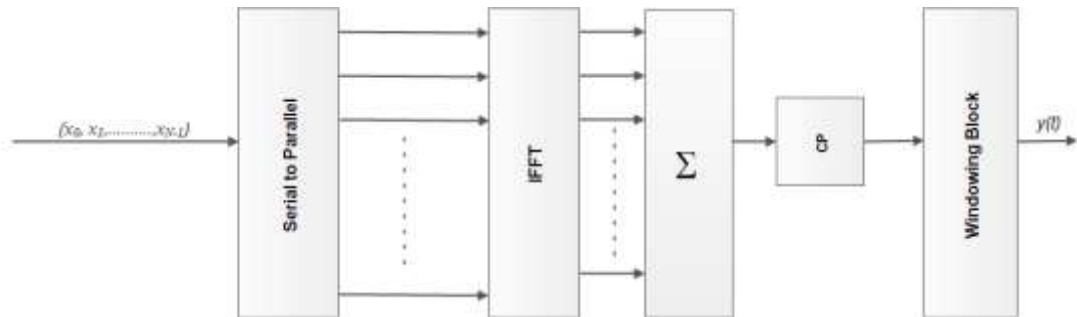
Figure 3.9. Symbol transitions in RC-windowed CP-OFDM.

Figure 3.10. Implementation of windowed CP-OFDM

arly with proportional to window interval length, N_w. Thus, the computational complexity presented by this technique is low compared to the other side lobe compression techniques discussed below. However, loses are induced in throughput as a result of the extended symbol period, and in power efficiency due to transmission of energy even during transition intervals [39]. But compared with basic CP-OFDM, RC time domain windowing results in clearly better suppression of side-lobes
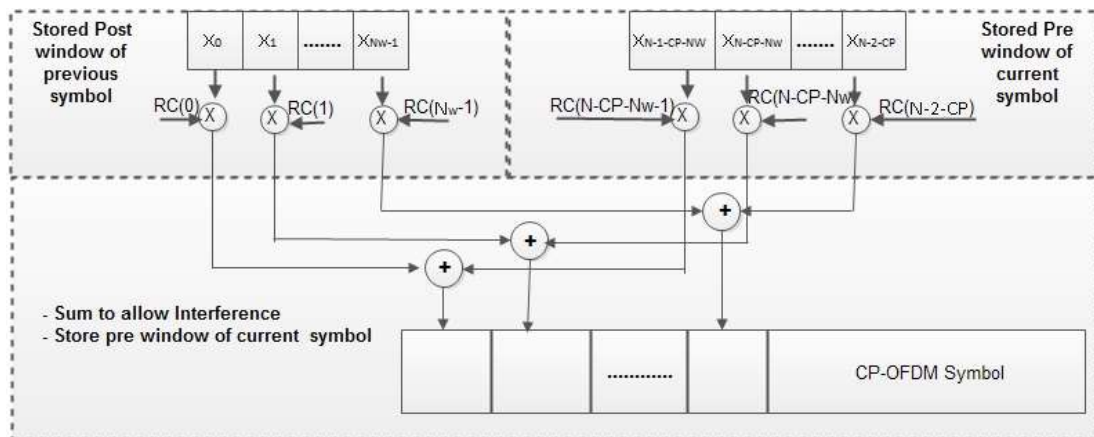

Figure 3.11. Window block structure.

which are far away from the active OFDM edges and this increases as the side lobe location gets further away. Nevertheless, the suppression of side-lobes by time domain windowing in useful band edges is considerably low.

3.3.3 Cancellation Carrier

Change in the input symbol values can change the power levels of OFDM side-lobes instantaneously. Cancellation carrier (CC) technique suppresses side lobe power at pre-defined range through the addition of weighted subcarriers in the deactivated band of the OFDM spectrum [40]. During implementation of CC factors like number of CCs, width of optimization range, and the scheme for CC weight calculations play important role on suppressing the side lobe power. Among these factors, the number of CCs and the optimization range are defined depending on system requirement along with affordable computational complexity. Nevertheless, weight evaluation is the main issue having major impact on the performance of this technique. The Figure 3.12 below explains the frequency representation used in CC. Optimization range is chosen as close as possible to useful band having high power side-lobes. Thus, CC has higher impact on side-lobes as near as it is placed.
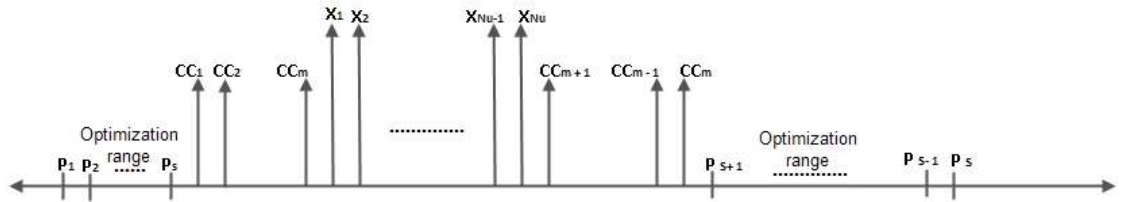

Figure 3.12. Frequency domain representation of OFDM spectrum using CC.

The number of CCs, M to be used needs to be identified prior to allocation of weights. In addition to location of each CC an IFFT input bin k should also be defined which is later used by subcarrier. Thus, an unweighted CC is modelled by sinc spectrum as in equation (3.27).

$$CC_k = sinc\left[T_s\left(f - \frac{k}{T_u}\right)\right] \tag{3.27}$$

After identification of unweighted CC optimization range point, S should be defined. Practically side lobe suppression can be applied to all points residing in the optimization range. This adds computational complexity to the system. Therefore, for the optimized use it is sufficient to implement optimization only in the middle between center frequencies of unused subcarriers. Thus, if we assume k active subcarrier then location of points for optimization is given by equation (3.28).

$$f = \frac{\frac{l}{2} + k}{T_u} \tag{3.28}$$

Here, l is an odd integer and value at that frequency is given by equation (3.29).

$$P_l = \frac{(-1)^{\frac{l+3}{2}} cos\left(l\frac{\pi}{2}\right)}{(1+q)\left(\frac{\pi}{2}l\right)} \tag{3.29}$$

Now, the side lobe power at OFDM spectrum at certain location k_s is given by equation (3.30).

$$P_s = \sum_{k \in A} \frac{x_k(-1)^{k-k_s+1}h_k}{(1+q)\left(k - k_s - \frac{1}{2}\right)\pi} \tag{3.30}$$

Here, A is set of active subcarriers and h_k is periodic function which changes as per active subcarrier index and optimization point index. After this the obtained optimization points are collected to form a column vector as $P = [P_1, P_2, \ldots \ldots P_s]^T$. Now, side lobe values at optimization points are collected. For unweighted CC they are calculated as:

$$C_{s,m} = \frac{(-1)^{k_m-k_s+1}h_{s,m}}{(1+q)\left(k_m - k_s - \frac{1}{2}\right)\pi} \tag{3.31}$$

A simple block diagram demonstrating OFDM with CC implementation is shown in Figure 3.12. Red arrow in the diagram denotes CC insertion. Weight evaluation block in the diagram adds computational complexity as discussed earlier to the system. This complexity can have high degree depending on CC scheme being implemented where complexity is defined by number of computations that needs to be done to solve weight of CC.

3.3.4 Subcarrier Weighting

Every subcarrier in OFDM is weighted by the IFFT input data symbol x_k varying instantly according to the information being sent. The subcarrier weighting (SW) technique multiplies each subcarrier by specific weights such that the side lobe power is decreased to a reasonable level [41]. Two parameters needed for subcarrier weight optimization are:
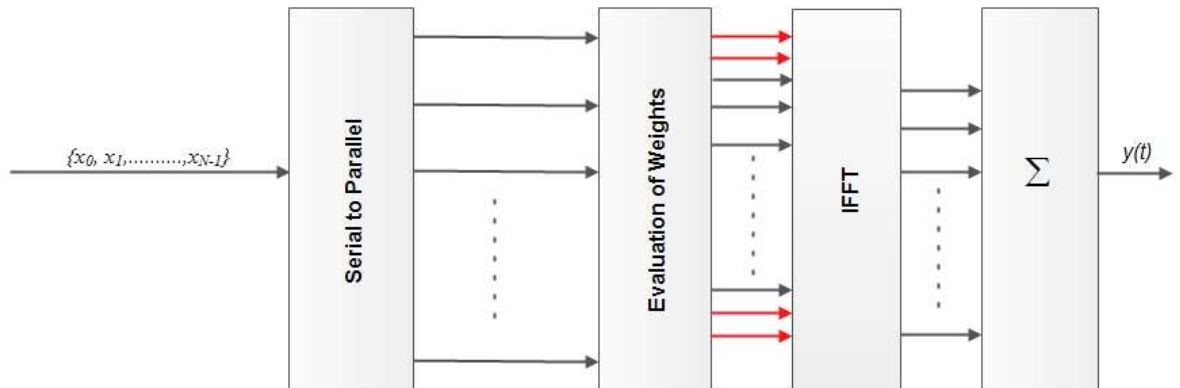
- Range of subcarrier weights
- Optimization range
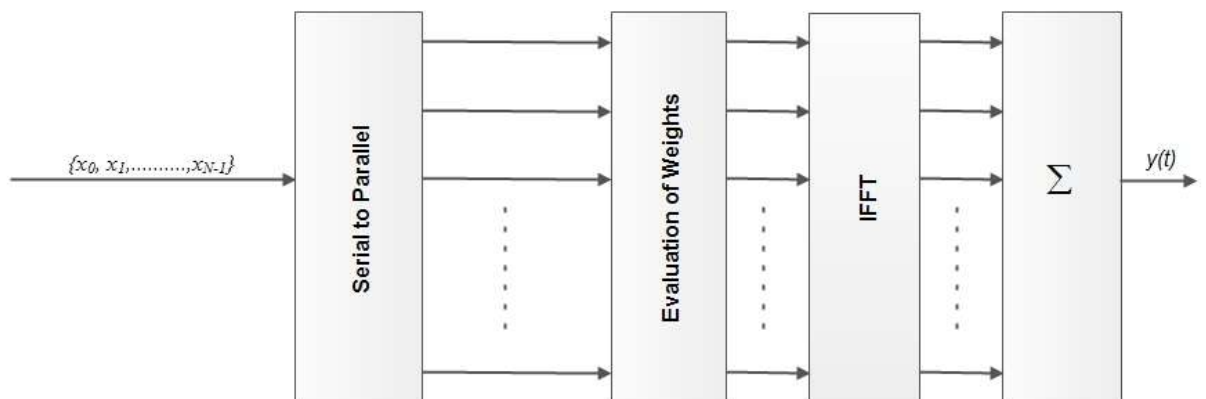

Figure 3.12. CC-OFDM implementation block

Figure 3.13. SW-OFDM implementation

SW implementation similar to CC technique is shown in Figure 3.13 where weighted subcarriers are produced by evaluation block and is fed for IFFT. This implementation results in much higher computational complexity than the CC technique due to non-linearity and size of the optimization problem.

In SW side information related to subcarrier weight is not transmitted because the effects of the weights are small enough to be modelled as random variations in the subcarrier symbols. This works well for low order constellations, BPSK or QPSK, or PSK type modulations. In those cases, the weighting does not affect the decision regions of the receiver, and just the variations of the subcarrier symbol powers affect the BER performance. However, for high order QAM constellations the weight range should be small and the side lobe suppression performance would be quite limited.

In the same way as in CC, the side lobe suppression performance of SW is high in the optimization range, whilst the performance outside the optimization range is weaker and approaches OFDM at far side-lobes. Hence, SW usage at narrow gaps is expected to be more efficient than in the guard bands of the overall spectrum.

3.4   Channel Estimation

In the OFDM receiver processing, knowledge of the channel for equalization is always required. Such information regarding the channel is obtained through the channel estimation process, which can be done in various ways: with the help of a parametric model, with the use of frequency or time correlation properties of channel, blind or pilot based and adaptive technique [42].

Non-parametric methods estimates the channel without relying on a specific channel model. On the other hand parametric estimation assumes a certain channel model and determines the parameters of this model. Thus based on these parameters quantities of interest are manipulated. Spaced-time and spaced-frequency correlations are specific properties of channel that can be incorporated in the estimation method, improving the quality of estimate. Pilot based estimation methods are the most commonly used methods which are applicable in systems where the transmitter emits some known signal. Blind estimation, on the other hand, relies on properties of signal and is rarely used in practical OFDM systems. Adaptive channel estimation methods are typically used for rapidly time-varying channels.

In this section, a pilot-based non-adaptive channel estimation method is elaborated which is used in this thesis as well. To estimate the channel, pilot symbols are required. An assumption that every P^{th} sub-carrier contains known pilot symbols $\left(X_{pk}\right)$ is done for this purpose. The pilot structures can be defined based on various structures as shown in Figure 3.14.

- An entire OFDM symbol may be allocated as pilot as shown in Figure 3.14 (a). Such an allocation will be highly beneficial for channel estimation in highly frequency-dispersive and low Doppler channels at the expense of sacrificing data rate [42].
- Pilots may be transmitted on individual sub-carriers during the entire transmission period as shown in Figure 3.14 (b). Such strategy is advantageous in moderately frequency-selective and high Doppler channels [42]. This pilot structure is used for this research as our transmission environment is frequency selective in nature.
- Pilots may be allocated in spaced intervals in time and frequency as illustrated in Figure 3.14 (c) and Figure 3.14 (d). Depending upon the time-frequency pilot spacing and channel properties, such an allocation strategy will work well in both high frequency-selective and high Doppler channels [42].

After FFT and CP (or zero-padding) removal, the received signal at pilot locations is extracted. Then using known pilot symbols $\left(X_{pk}\right)$ and the corresponding received sample values $\left(Y_{pk}\right)$ at those pilot subcarriers, the calculations for the raw channel estimate $\left(H_{pk}\right)$ at pilots is done as follows:

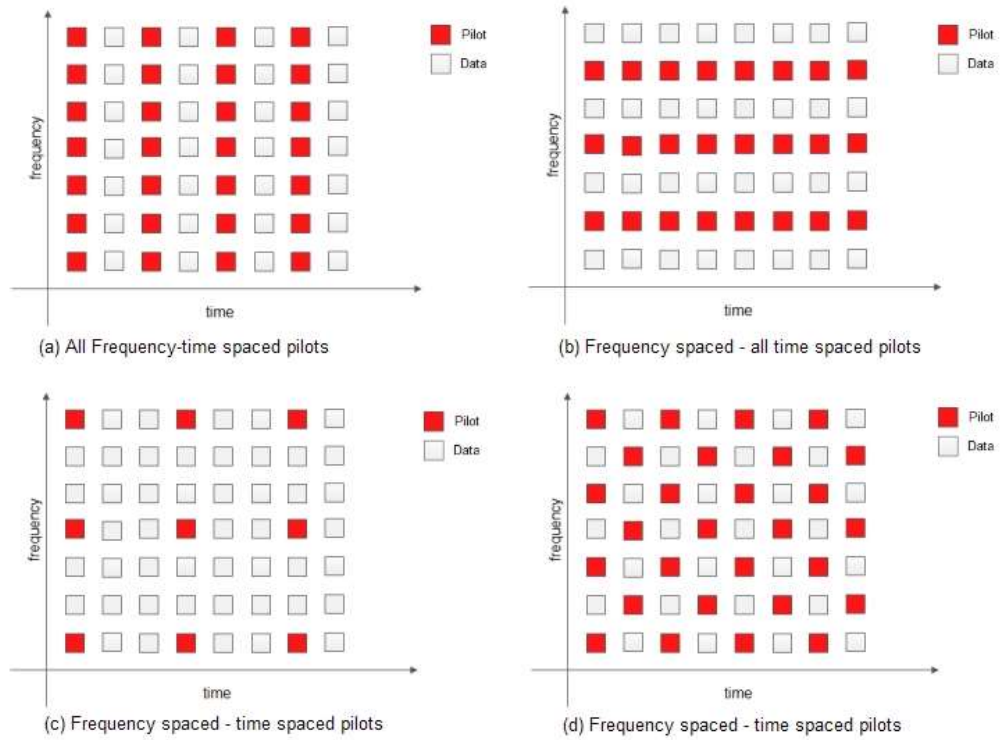$$H_{pk} = \frac{Y_{pk}}{X_{pk}}. \tag{3.32}$$
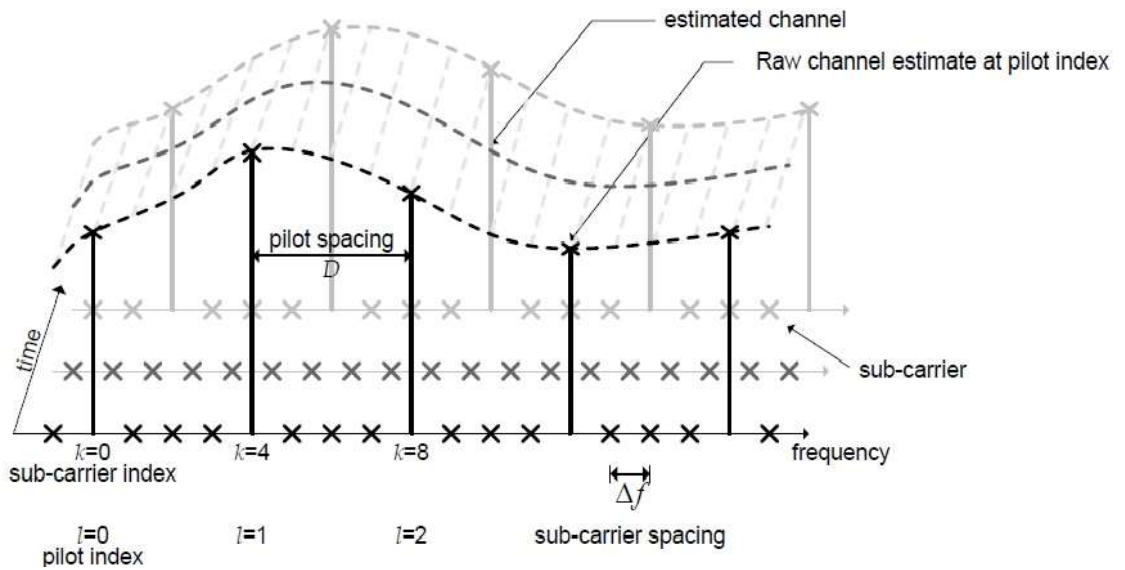
Figure 3.14. Pilot structure definitions

Figure 3.15. Channel estimation by linear interpolation

Different methods can then be applied to estimate the channel over all sub-carrier frequencies [42].

Channel estimation in OFDM is a two-dimensional (2-D) problem i.e., the channel needs to be estimated in time-frequency domain as shown in Figure 3.15. Hence 2-D filtering methods could be applied for estimating the channel from pilots. However, due to the computational complexity of 2-D estimators, the scope of channel estimators can

be limited to one-dimensional (1-D). The idea behind 1-D estimators is to estimate the channel in one dimension and later estimate the channel in the second dimension, thus obtaining a 2-D channel estimate. Channel estimation methods, 2-D or 1-D dimensional, can be characterized into three types [42]:

- Simple linear interpolation.
- Generalized linear network models based on orthogonal polynomials (least-squares method).
- Wiener filtering using second-order statistics of the channel (LMMSE method).

The focus of this report has been on 1-D methods, where we apply channel estimation in frequency domain first, and later use interpolation based on linear interpolation method averaging between two pilot positions.

4 SYSTEM MODEL

This chapter lays out fundamental background on the PLC system model that has been considered in this thesis. This chapter gives brief insight of system model, defining channel model of the automotive environment, interference and noise model that occurs in the vehicular environment, OFDM symbol block structure, the pilot structure for channel estimation, and repetitive coding scheme with maximum ratio combining technique.
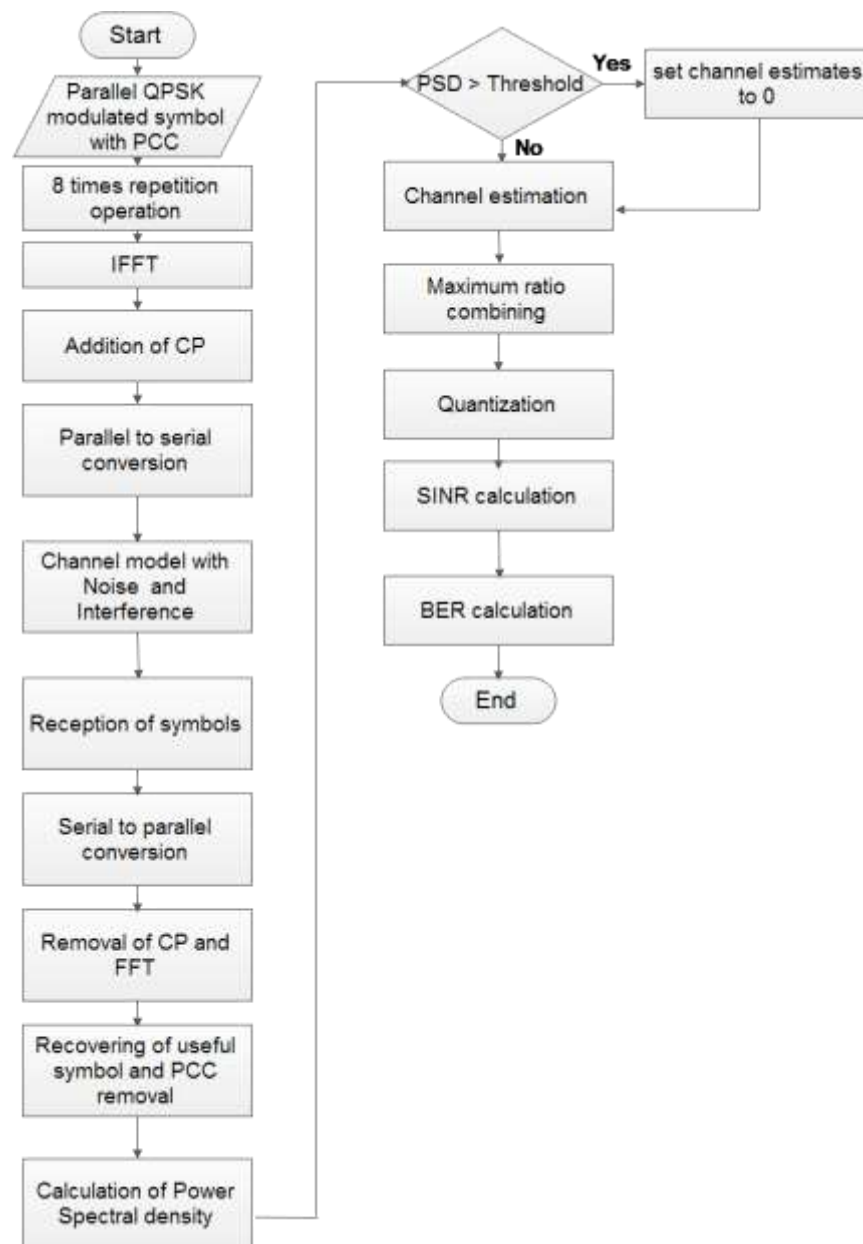

Figure 4.1. Simulation flowchart.

As an approach of simulation for research consideration first a basic simulation is done. After study of thus obtained results further consideration for robust communication is made and hence simulation is carried out for the different scenarios. The results of the simulations will be discussed in the chapter to follow. The simulations for this thesis work flow the system model as shown in Figure 4.1. The implementation of the OFDM model is based on the OFDM basic theory and comprises of all the essential components.

4.1   Channel Model

Modelling of automotive environment channel is heavily based on investigation done on the properties of the vehicular DC-wire for the purpose of data communication in cars [7]. The author of this study has aimed to model the transmission channel representing DC-wires in automotive environment. In a modern car large number of DC cables following different routes exist. These cable routes differ from car to car. Thus, as a fundamental approach of measurement between transceiver and receiver with $2\ m$ and $8\ m$ distance scenario between them has been done with the help of a network analyzer in the automotive environment [7].
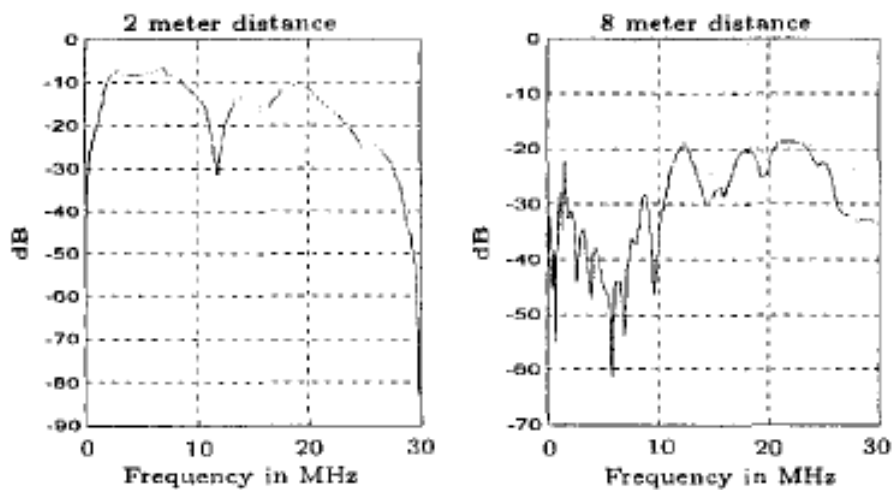

Figure 4.2. Transfer functions for DC wires in a car [7]. (a) 2 m route. (b) 8 m route.

The results are shown in figures 4.2 (a) and 4.2 (b). Fading of various frequency components due to reflections in the cable were observed in the measurements. These fading effects were results of unadapted terminations in the DC-wires. The magnitude of the transfer function delivers some useful results in the form of frequency segments where reliable communication can be performed in the automotive environment. Thus, based on these results, it is obvious that a reasonable data transfer can be achieved above the frequency band of $10\ MHz$ where the transfer function of channel has relatively flat response. In any case, the channel is highly frequency selective, as expected.

In contrast to the frequency domain consideration, the impulse response is another important factor. The impulse response function determines required CP length in OFDM transmission. Thus, the channel impulse response was calculated from the transfer function based on inverse Fourier transform. Figures 4.3 (a) and 4.3 (b) show the impulse response corresponding to the channel transfer functions of Figures 4.2 (a) and 4.2 (b). The impulse response in Figure 4.3 (a) and 4.3 (b) shows that after $40\ \mu s$, the impulse response for $8\ m$ route completely fades away. On the other hand, the impulse response for $2\ m$ route faded away in just $0.2\ \mu s$. Considering both impulse responses, it is significant to consider the worst case scenario addressing the transfer channel for all available cable routes in automotive environment. Therefore, it can be concluded that for bit rates above $250\ kbits/s$, equalizer is required to combat against ISI [7].
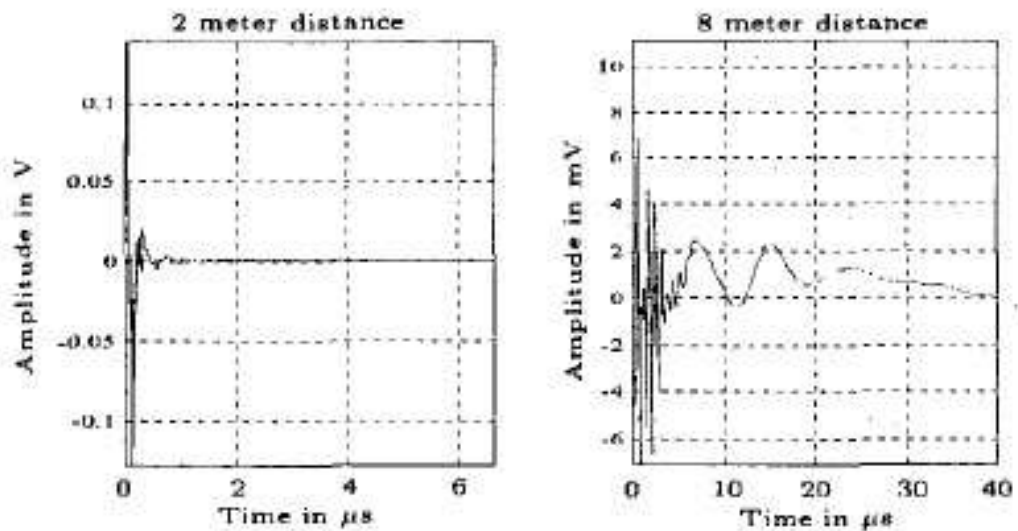

Figure 4.3. Impulse responses for DC-wires in a car [7].
(a) 2 m route. (b) 8 m route.

4.2 Interference and Noise Model

Interference and Noise model considered in this thesis is obtained from measurement campaign done in a compact electrical car [8]. The measurement campaign was carried out focusing on the noise and channel response for both the narrow band range of $30\ kHz$ to $500\ kHz$ and the broad band range of $2\ MHz$ to $100\ MHz$. This measurement produced the results where it is seen that electrical power drivers and DC/DC convertor produces high noise which are more pronounced in low frequency spectrum at low frequencies.

The measurement was done in a 4-wheel compact electrical car having two 3-phase brushless $48\ V$ engines and four $12\ V - 100\ Ah$ lead gel batteries. The battery pack directly supplies power to two ECUs driving electric engines in this car. The rotation of electric engine rotor is ensured by commutation of power through the three phases ac-

cording to the control sequence. A DC/DC converter is used to convert $48\,V$ DC to $12\,V$ DC, in order to supply the $12\,V$ power network of the vehicle. The $12\,V$ electrical system feeds the $12\,V$ standard peripherals, i.e., lights, break lights, turn lights, etc.

Figure 4.4 and Table 4.1 defines the measurement scenario for this measurement campaign. To measure the results in this environment a Digital Storage Oscilloscope (DSO) was used. The test connectors were placed in parallel to feeding conductors of peripherals without disconnecting them from power grid. A built in connector was used to replace the corresponding fuse inside the fuse box, as shown in measurement setup. This built in connector acts like a shunt connector and at the same time gives access to the test nodes. The measurement has been done for three states of the vehicle:

- Engine is OFF and front and rear position lights are switched ON.
- Engine is ON with no loads.
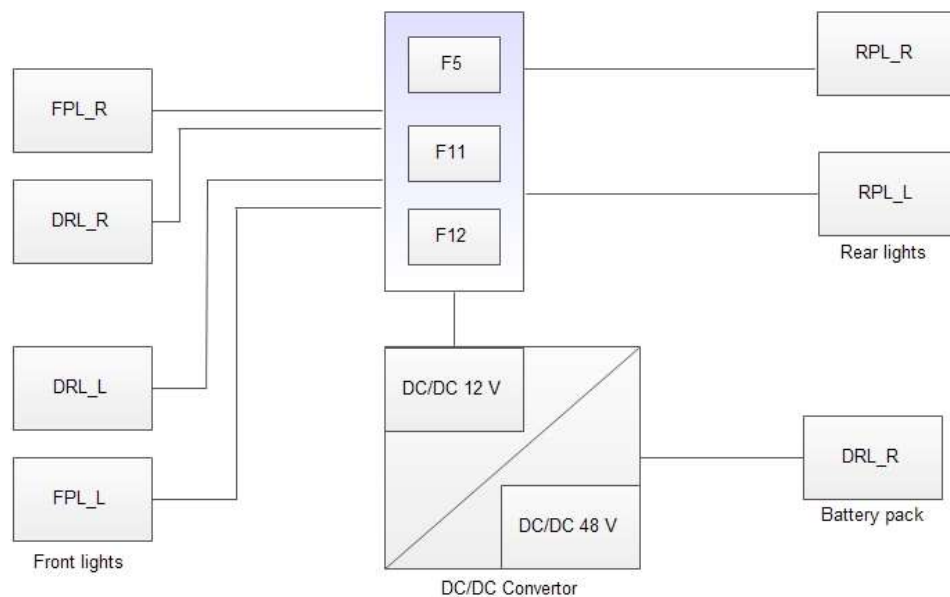- Engine is turned with heavy load situation.

Figure 4.4. Measurement setup.

With this measurement setup, the main source of noise in this environment was found to be the DC/DC converter. The switching DC/DC converter had two reactive components, typically an inductor and a capacitor connected in the form of LC low pass filter, a MOSFET used as a switch and a diode. This MOSFET was driven by square wave with specified duty cycle to provide required conversion ratio. When square wave was high, input voltage charged inductor and diode was turned OFF. The situation was vice-versa for low voltage level. Thus, the result at output was a constant voltage with triangular ripple caused by the charging and discharging of the inductor. This results in mea-

Table 4.1 List of test points

Test Point	Acronym
Front position light, left	FPL_L
Daytime running light, left	DRL_L
Front position light, right	FPL_R
Daytime running light, right	DRL_R
Rear position light, left	RPL_L
Rear position light, right	RPL_R
Battery pack (48 V)	BP
DC/DC converter (48 V side)	DC/DC48
DC/DC converter (12 V side)	DC/DC12
Fuse brake lights	F5
Fuse FPL_L-RPL_R	F11
Fuse FPL_R-RPL_L	F12

sured noise with triangular waveform having additional resonating effect. At the falling and rising edges of square wave an overshooting response was added to triangular ripple voltage. The result measured at DRL_L access point is shown in Figure 4.5. The figure depicts an over shooting element limited to small voltage value with superposition of another noise component at high loading condition of the engine. The analytical expression for this triangular noise is:

$$f_{tri}(t) = \sum_{k=1}^{\infty} a_k^{(tri)} \cos\left(\frac{2\pi t}{T_{DC}} k\right) + b_k^{(tri)} \sin\left(\frac{2\pi t}{T_{DC}} k\right) \tag{4.1}$$

Where,

$$\begin{cases} a_k^{(tri)} = \dfrac{A_{tri}}{k\pi^2}\left[\dfrac{1}{D_{DC}}\left[\cos(2\pi k D_{DC}) - 1\right]\right] \pm \dfrac{1}{1 - D_{DC}}\left[1 - \cos(2\pi k D_{DC})\right] \\ b_k^{(tri)} = \dfrac{A_{tri}\sin(2\pi k D_{DC})}{\pi^2 k^2 D_{DC}(1 - D_{DC})} \end{cases}$$

The triangular noise in the measurement had period of $T_{DC} = 15.4\ \mu s$ with duty cycle of $D_{DC} = 0.37$.

Another noise source in this environment was power signal fed to the engines. Heavily loaded engines demand a great deal of current. This current is composed of the square waveform. This current generates a magnetic field that is concatenated with the rest of the electrical power system. This induced a noise voltage on other wires depending on load at the engine with amplitude of A_{sq}. The Fourier expansion for the concatenated voltage is shown in equation (4.2). Figure 4.6 depicts the square waveform that was measured on a solenoid wrapped on the phase wire.

$$\tag{4.2}$$

$$f_{sq}(t) = \sum_{k=1}^{\infty} a_k^{(sq)} \cos\left(\frac{2\pi t}{T_{EN}}k\right) + b_k^{(sq)} \sin\left(\frac{2\pi t}{T_{EN}}k\right)$$

Here,

$$\begin{cases} a_k^{(sq)} = \dfrac{A_{sq}}{k\pi} \sin(2\pi k D_{EN}) \\ b_k^{(sq)} = \dfrac{A_{sq}}{k\pi} [1 - \cos(2\pi k D_{EN})] \end{cases}$$

Here, the measure square noise had period of $T_{EN} = 25\ \mu s$ with duty cycle of $D_{EN} = 0.67$.
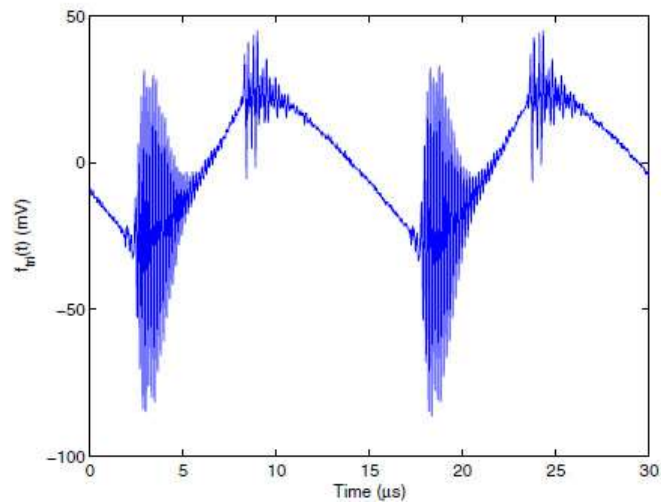

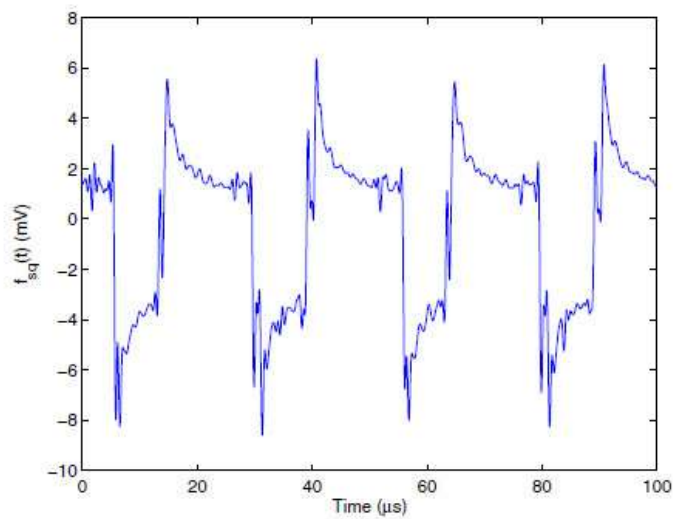*Figure 4.5. Noise voltage waveform under heavy load condition of engine [8].*

Figure 4.6. Measured Square noise on solenoid wrapped on a phase [8].

4.3   OFDM Symbol

After a thorough consideration of the channel and interference model in automotive environment, a robust CP-OFDM transmission system was designed in this work. The symbols are QPSK modulated complex symbols. The parameters for the OFDM signal are shown in Table 4.2 and the OFDM symbol block is depicted in Figure 4.7. The parameterization is inspired from the HPAV system. The subcarrier spacing is the same, but the sampling rate is reduced from 75 MHz to 50 MHz. The choice of active subcarriers is based on the channel properties as it was distinguished to perform well above the frequency band of 10 MHz. Also the interferences are at a lower level at higher frequencies. PCC has been implemented as a major element of the proposal to achieve a reasonable suppression of side-lobe power. Even more importantly, PCC processing on the receiver side suppresses effectively interfering spectral components at near-by frequencies to a subcarrier. The number of QPSK data symbols modulated to an OFDM symbol is limited to 25. After implementation of PCC the number of subcarriers is doubled to 50. After repetition coding by 8 times, the number of active subcarriers becomes 400. With 400 subcarriers communication in the frequency band above 10 MHz is achieved. The length of cyclic prefix of 512 is used to maintain orthogonality between subcarriers based on the basic OFDM theory. With these parameters, and taking into account the pilot structure (one out of three symbols is a pilot) the raw bit rate of the PLC link is about 651 kbps, which is quite sufficient for the intended application.

Table 4.2: OFDM parameters

Parameter	Value
Sampling Frequency	50 MHz
FFT length	2048
Subcarrier modulation	QPSK
Active subcarrier frequency range	10 MHz to 20 MHz
Number of useful subcarrier symbol streams	25
Number of symbols per transmission frame	100
Side lobe power suppression, PCC	Yes
Number of subcarrier after PCC	50
Repetition coding factor	8
Number of subcarrier after repetition coding	400
Cyclic Prefix length, 2048/4	512

4.4   Pilot Structure

All frequency spaced-time spaced pilot structure as described in chapter 3.4 is used. As shown in Figure 4.8, pilots in the form of known symbol starting from first subcarrier with step size of 3 has been taken till the end of useful subcarriers. This pilot structure has been designed for robust channel estimation and low computational complexity during the channel estimation process. It is expected that the pilot density could be signifi-

cantly reduced without affecting the system performance. However, the optimization of the pilot structure remains as a topic for future studies.
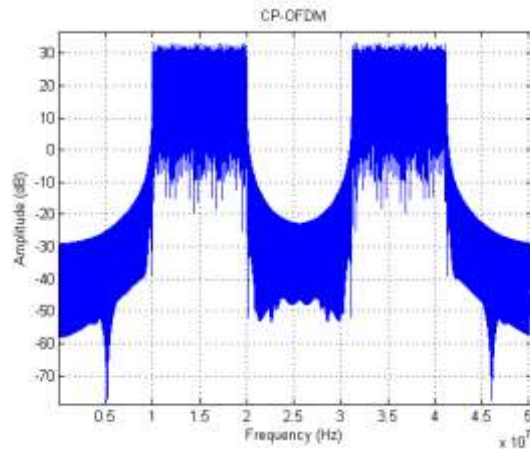

Figure 4.7. Transmitted spectrum of the proposed robust CP-OFDM symbol for PLC. The discrete-time spectrum is shown, the periodic image of the OFDM signal is suppressed by an analog filter in the transmitter.
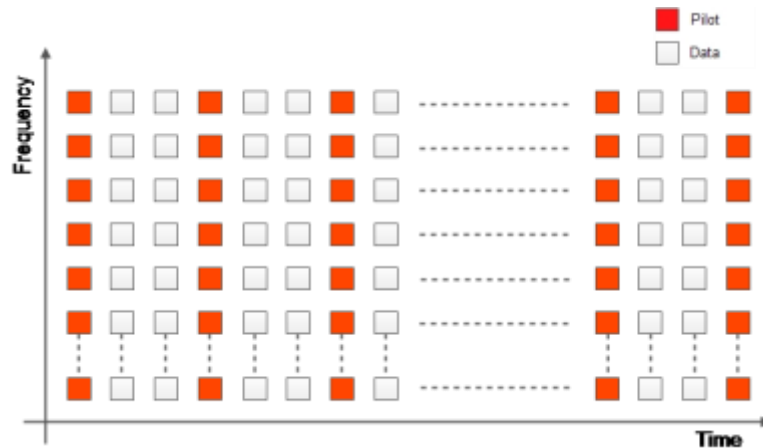

Figure 4.8. Pilot structure.

4.5 Channel Estimation and Quantization

In channel estimation process, the channel estimates for the pilot locations are calculated first. For the respective position of pilots, X_{pk} the channel estimates are calculated by dividing the received sample value by the corresponding pilot symbol value as according to equation (3.32).

After calculation of the channel estimates at the pilot locations, channel estimates for the data symbol positions are obtained through linear interpolation as follows:

$$H_{i,k} = \frac{2 * H_{i,k-1} + H_{i,k+2}}{3}, \text{for } k = 2,5,8, \dots \tag{4.3}$$

$$H_{i,k} = \frac{H_{i,k-2} + 2 * H_{i,k+1}}{3}, \text{for } k = 3,6,9, \dots \tag{4.4}$$

Here, i is the subcarrier index and k is the OFDM symbol index.

Using linear interpolation for channel estimation relieves from complex computation with reliable estimates as a result.

4.6 Detection and Repetition Coding

The data symbol estimates are obtained by dividing the corresponding received sample value with the corresponding channel estimate. The data symbols are then detected by choosing the closest constellation point according to the Euclidean distance criterion. Extremely low channel estimate for a subcarrier indicates that the detected symbols are not likely to be reliable. Repetition coding enables us to send the same data symbols over several subcarriers, introducing frequency diversity, and provides robust transmission with low complexity receiver processing. Therefore, after channel estimation maximum ratio combining (MRC) of the received repeated symbols is used to maximize the SNR in symbol detection.

The baseband signals in different diversity subcarriers is expressed as:

$$r_i(t) = g_i x(t) + n_i(t) \tag{4.5}$$

Here, $n_i(t)$ are independent complex White Gaussian noise processes having equal variance. The output of linear combiner can now be expressed as:

$$y(t) = \sum_{i=1}^{L} w_i(g_i x(t) + n_i(t)) = x(t) . \sum_{i=1}^{L} w_i g_i + \sum_{i=1}^{L} w_i n_i(t) \tag{4.6}$$

The instantaneous signal and noise powers at the combiner output now becomes:

$$\sigma_y^2 = E[|x(t)|^2] . \left| \sum_{i=1}^{L} w_i g_i \right|^2$$

$$\sigma_{nc}^2 = \sigma_n^2 . \sum_{i=1}^{L} |w_i|^2 \tag{4.7}$$

Thus, the SNR at the combiner output can now be calculated as:

$$\gamma_c = \gamma_{av}.\frac{\left|\sum_{i=1}^{L} w_i g_i\right|^2}{\sum_{i=1}^{L} |w_i|^2} \tag{4.8}$$

Here, γ_c is instantaneous SNR of combiner output and γ_{av} is the average SNR which is assumed to be equal for all the subcarriers. Now, by Schwarz inequality law:

$$\left|\sum_{i=1}^{L} w_i g_i\right|^2 \leq \sum_{i=1}^{L} |w_i|^2 . \sum_{i=1}^{L} |g_i|^2 \tag{4.9}$$

Above equation holds equality when $w_i = cg_i^*$, where c is an arbitrary complex constant. The instantaneous SNR is maximum, when $c = 1$. Thus, the maximum SNR due to MRC is:

$$\gamma_{MRC} = \gamma_{av}.\sum_{i=1}^{L} |g_i|^2 = \sum_{i=1}^{L} \gamma_i \tag{5.1}$$

Here, γ_i is the instantaneous SNR at i^{th} subcarrier [43].

The health of each used subcarriers is tested by estimating the received power of each subcarrier over each data frame. If the subcarrier power level is exceptionally high, the subcarrier is considered to be destroyed by interference and is not used for detection. This can be implemented simply by using a zero weight for all those subcarriers in the MRC. The decision about interfered subcarrier is based on a threshold for the power level, which is obtained experimentally through simulations. The simulation results of SER and MSE when threshold value is increased for repetition coding factor of 4 is shown in the figures 4.9 (a) and 4.9 (b). The figures 5.1 (a) and 5.1 (b) shows the results for repetition coding factor of 8. On increasing the threshold limit both MSE and SER are found to increase. The analysis was done for +2 dB, +3 dB and +4 dB from the minimum PSD of active subcarriers at receiver as threshold values. Among the chosen threshold limits, the limit of +3dB had optimum results for MSE and SER for both repetition coding factors. The average SER was below 0.05 with average MSE of almost -9.8 dB for repetition factor of 4, whereas average SER of 0.028 and 0 dB average MSE was achieved with the same threshold limit of +3 dB for repetition factor of 8. Thus, further analysis on the simulation is based on threshold limit of +3 dB.
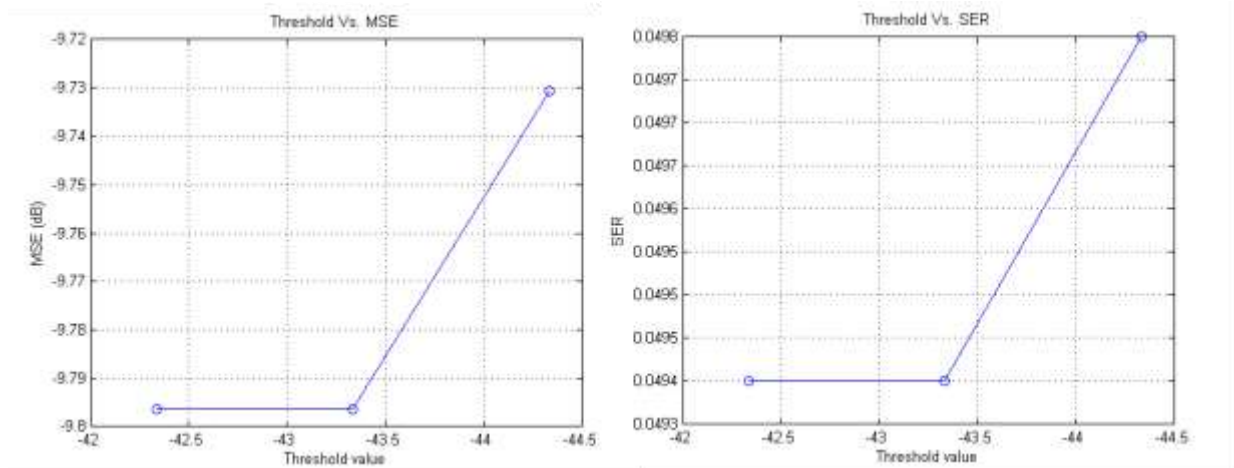
Figure 4.9. MSE and SER vs. threshold for repetition coding factor of 4.
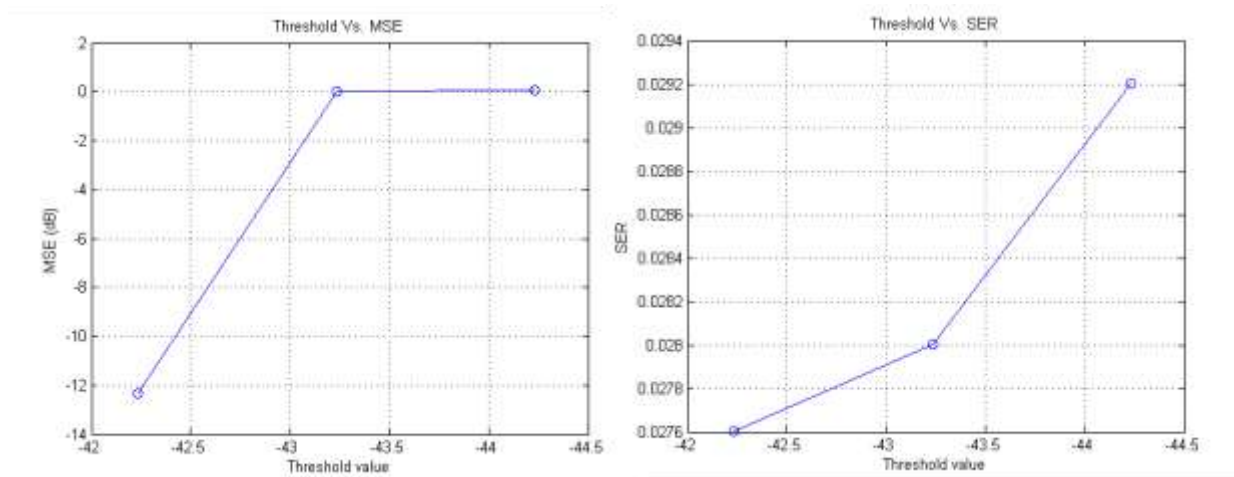*(a) MSE. (b) SER.*

Figure 5.1. MSE and SER vs. threshold for repetition coding factor of 8.
(a) MSE.   (b) SER.

4.7   Symbol Error Rate

After detecting the received symbols, the final stage for verification of system function-ality is based on symbol error rate (SER) calculation. Symbol error rate is calculated as:

$$Symbol\ error\ rate = \frac{total\ number\ of\ errornous\ symbols}{total\ number\ of\ subcarriers}. \tag{5.2}$$

5 SIMULATION RESULTS

This chapter describes the results of simulation based evaluation of the proposed robust OFDM system design for automotive PLC communication. The interference model as discussed in Section 4.2, with SIR level of -25.22 dB, and frequency selective channel model from section 4.1 are considered to obtain the results discussed in this chapter. The threshold value of +3 dB as calculated from the simulation results in Section 4.6 is also considered for the analytical part. First of all the results from preliminary simulation study is analyzed. In the preliminary study there was no implementation of error control mechanism and side lobe power suppression technique. After the analysis done, based on the results of this preliminary study enhanced OFDM system parameters are determined. The enhanced OFDM system thus designed is robust against the strong interference in the automotive environment for PLC in automotive environment. The results of enhanced OFDM system is presented in a precise analytical manner in this chapter.

5.1   Preliminary Simulation Results

As discussed in section 4.3, for preliminary assessment of PLC in automotive environment, an OFDM system with properties stated in Table 5.1 was considered. The output of this simulation is presented in Figure 5.1, 5.2, 5.3 and Figure 5.4.

Table 5.1: OFDM parameters for preliminary study

Parameter	Value
Sampling Frequency	50 MHz
FFT length	2048
Subcarrier modulation	QPSK
Active subcarrier range	10 MHz – 20 MHz
Number of useful subcarrier	400
Number of symbols per frame	100
Side lobe suppression	No
Repetition coding	No
Maximum ratio combining	No
Length of cyclic prefix	512

The resulting baseband OFDM signal spectrum is shown in Figure 5.1. Figure 5.2 demonstrates received PSD at frequency band of the active subcarriers without interference. All the subcarriers are received at uniform power range within -46.3 dB to -46.54 dB. After addition of interference model of Section 4.2, PSD of the active signal band is

depicted in Figure 5.3. It is seen that most of the subcarriers are severely affected and have a low signal to interference plus noise ratio (SINR), resulting in high SER at the receiver as shown in Figure 5.4, where 65% to 87% of symbols are lost.
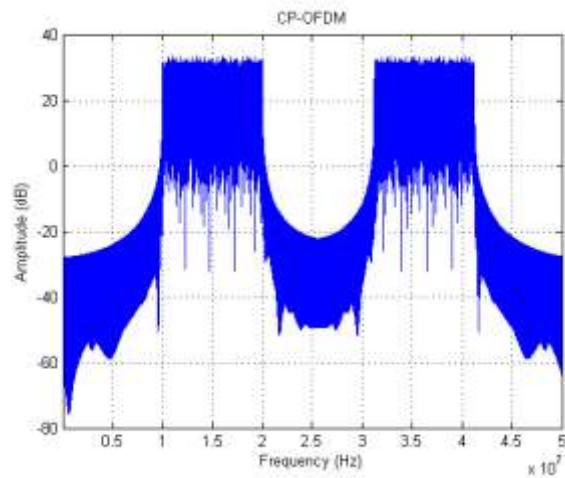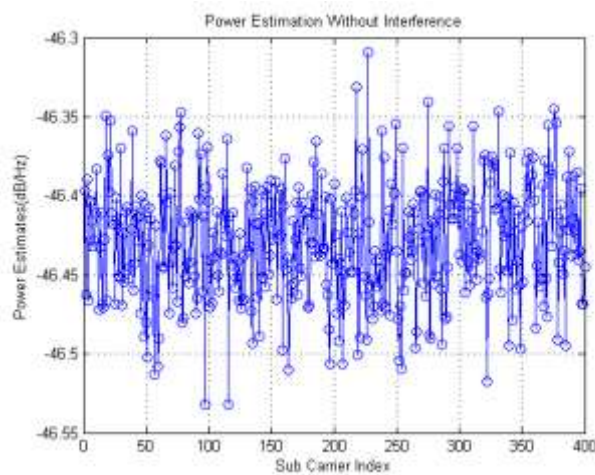

Figure 5.1. Preliminary CP-OFDM symbol block.

Figure 5.2. PSD of received symbols without interference.
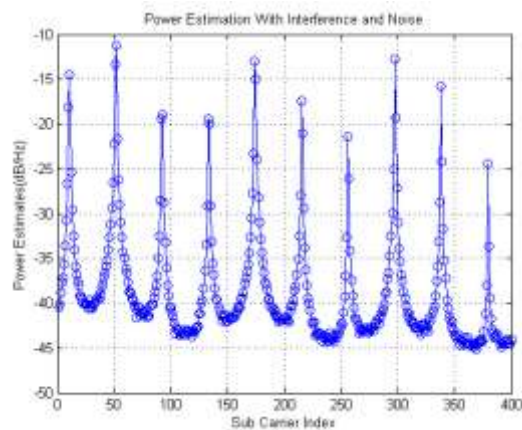

Figure 5.3. Noise PSD of received active subcarriers in the presence of square wave interference in the basic OFDM system.
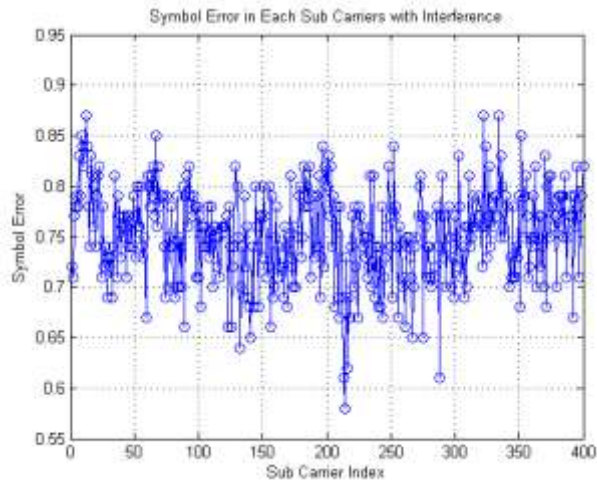
Figure 5.4. Symbol error rate in subcarriers in the presence of square wave interference in the basic OFDM system.

With this preliminary study of PLC communication in automotive environment, it was concluded that interference is too high for a reliable PLC communication using the basic CP-OFDM setup. Due to the interference leakage, large number of subcarriers are damaged. Thus, to overcome these problems, the following issues should be taken into account to enable robustness for PLC in automotive environment:

- Side lobe power suppression technique should be used to suppress high side lobe power. This is important particularly on the receiver side to suppress the leakage from the harmonic spectral components of the interference.
- Error control coding should be used to ensure recovery of lost symbols due to damaged subcarriers. Repetition coding was selected as a simple low-complexity scheme. Since we are not targeting at very high data rates, the resulting quite significant overhead in data rate can be tolerated.
- Maximum ratio combining should be used for detection to maximize the signal to noise ratio and link performance. In this context, it is important to identify the damaged subcarriers and suppress them from the detection process.

5.2   Enhanced OFDM System Simulation Results

To implement aforementioned considerations, an enhanced OFDM system model has been developed according with parameters as stated in Table 5.2. To overcome the effect of high side lobe power, PCC was chosen as the side lobe power suppression technique for further implementation. The effect of PCC is studied and the results are discussed below. Repetition coding with MRC based detection is another key element to improve robustness. Thus, repetition coding of factor 4 and 8 are simulated to see the effect. After analyzing the results of both repetition factors it is seen that repetition cod-

ing factor of 8 has more profound robustness against the strong interference decreasing the SER with low MSE.

When interference was applied to the enhanced OFDM symbols with PCC and repetition coding there was a clear improvement in the output of signal processing results. Resulting performance is demonstrated in the Figure 5.5. As seen in Figure 5.5 concerning the PSD of active subcarriers, a lower number of subcarriers are damaged, because PCC reduced the power leakage from the narrow band interferences to the useful subcarriers. Repetition coding enabled us to reduce the MSE and SER compared to the system with no repetition coding.

Table 5.2: Enhanced OFDM parameters

|	*Case I*	*Case II*
Parameter	***Value***	***Value***
Sampling Frequency	50 MHz	50 MHz
FFT length	2048	2048
Subcarrier modulation	QPSK	QPSK
Active subcarrier range	10 MHz – 20 MHz	10 MHz – 20 MHz
Number of symbols	100	100
Repetition factor	4	8
Number of useful subcarrier	50	25
Number of subcarrier after PCC	100	50
Total number of active subcarriers	400	400
Side lobe power suppression, PCC	Yes	Yes
Cyclic Prefix length, 2048/4	512	512
Data rate	1302 kbps	651 kbps
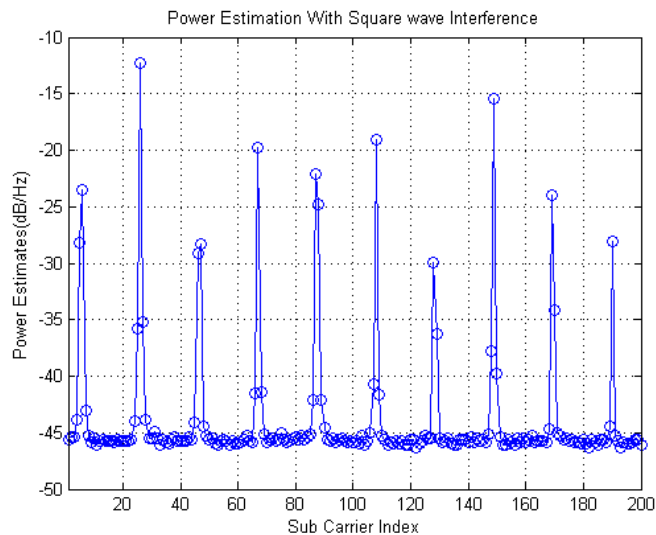
Figure 5.5. Noise PSD of received active subcarriers in the presence of square wave interference in the enhanced OFDM system.

The ability of the system to recover damaged symbols from healthy subcarriers has reduced SER drastically resulting in low MSE in all data streams. The results are shown in Table 5.3 for MSE and SER, where the effect of PCC and repetition coding implementation is seen. On the other hand, the data rate is reduced by the factor of 2 on increasing the repetition coding factor. In practice, the choice of the repetition factor depends on the requirements of the application and on the additional error control coding to be included in the system.

Thus, based on the above results and discussion, it can be concluded that implementation of side lobe power reduction technique and repetition coding with MRC has a fruitful result on encountering interference in automotive environment.

Table 5.3: Effect of PCC and repetition coding on MSE and SER

Values	Case I	Case II
Repetition factor	4	8
Number of damaged subcarriers	26	26
Average MSE	-9.73 dB	-11.83 dB
Average SER	0.049	0.0304

5.3   Effect of Interference Power Level

The dependency of the interference power level and enhanced OFDM system performance on the varied interference power level is studied here in this section. The interference power level is now varied from 10 dB stronger to 10 dB weaker (with respect to the cases shown above) with step size of 5 dB.

The power spectrums of active subcarriers at the receiver simulated with different interference power levels are shown in figures 5.6 (a), 5.6 (b), 5.6 (c) and 5.6 (d). The effect of varied interference power level is further analyzed with effect seen on MSE and SER parameters. The Table 5.4 below shows the effect on MSE and SER due to variation in interference power levels.

Table 5.4: MSE and SER with varied interference power levels.

Parameter	MSE	SER
10 dB stronger (SINR = -34.83 dB)	-0.61 dB	0.35
5 dB stronger (SINR = -24.85 dB)	-5.94 dB	0.10
0 dB stronger (SINR = -14.84 dB)	-11.83 dB	0.0304
5 dB weaker (SINR = -4.86 dB)	-30.96 dB	0
10 dB weaker (SINR = 5.13 dB)	-36.33 dB	0

Increased interference power level increased MSE and SER in the active subcarriers at the receiver end. But MSE and SER are drastically reduced with weaker interferences. It can be said that with the relative interference levels above 0 dB, the performance is severely damaged, and the practical limit for the feasibility of the proposed scheme is a few dB above the 0 dB reference level.
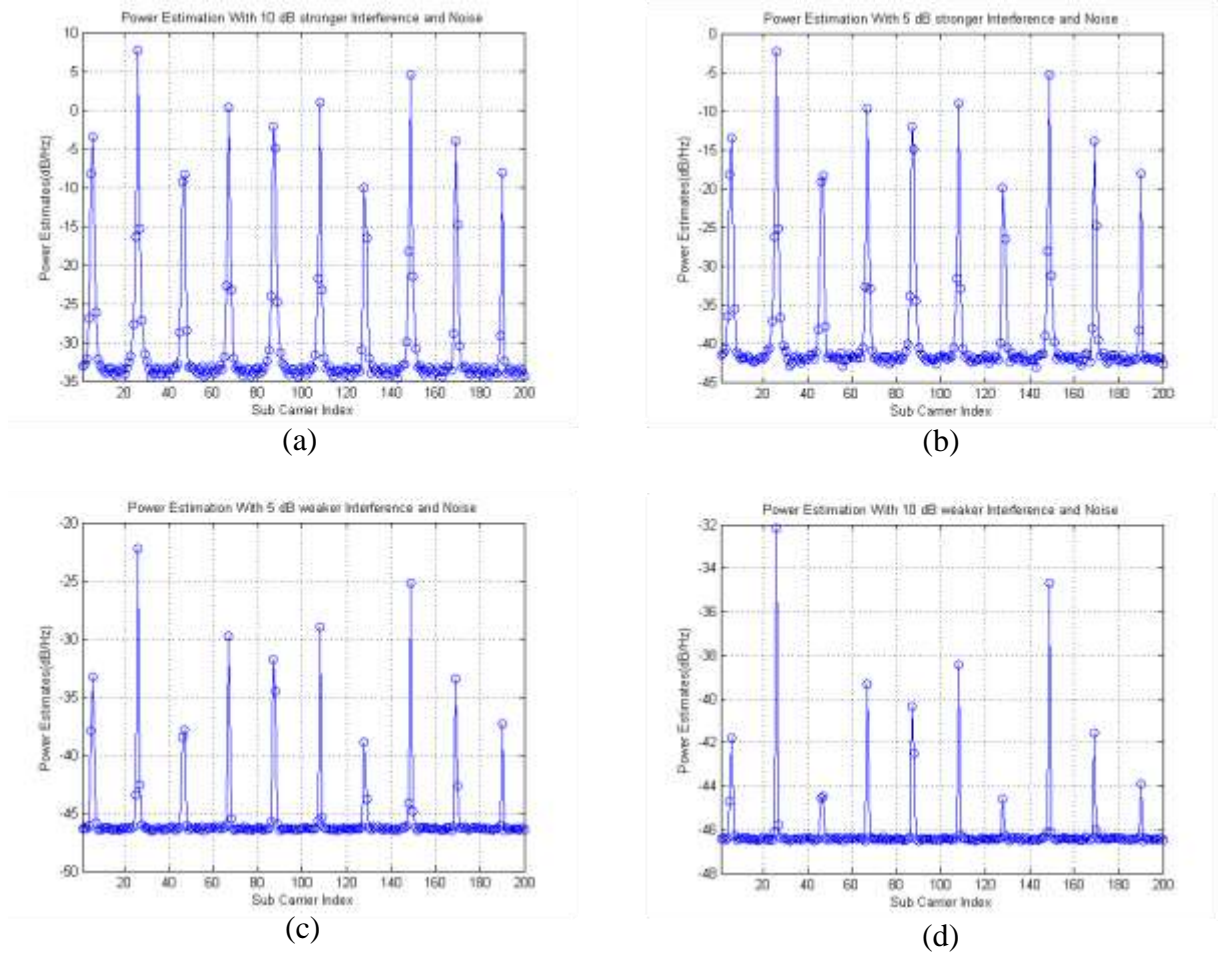

Figure 5.6. Noise PSD of received active subcarriers with varied interference power level in the enhanced OFDM system. (a) 10 dB stronger interference (b) 5 dB stronger interference (c) 5 dB weaker interference (d) 10 dB weaker interference.

The use of additional strong error control mechanism is required for 5 dB stronger interference to improve the SER, making PLC possible in this condition. Furthermore, with reduced interference power levels the environments are favorable for PLC in automotive domain. The bit error rate (BER) can fairly be assumed to be SER/2, as QPSK scheme has been used for subcarrier modulation in this enhanced OFDM system.

6 CONCLUSION AND FUTURE WORK

A study for PLC in the automotive environment with realistic frequency selective channel and interference models was done in this thesis. Due to the constantly high interference occurring in this environment a straight forward communication link design was not possible. Therefore, a robust enhanced OFDM system was proposed.

Frequency selectivity in the channel is high. To encounter the frequency selectivity of the channel, CP-OFDM is utilized due to its robustness against frequency selectivity. Due to high interference level, the power leakage from narrowband interferences was high, thus PCC with OFDM was implemented to suppress this high side lobe power. With less power leakage, a lower number of subcarriers were damaged resulting into low SER. Concluding with the obtained results, the proposed enhanced OFDM system had sufficient data rate for most of the monitoring and controlling functions. But the data rate achieved with this system is not enough for systems like infotainment.

Within the frame work of this thesis, OFDM system with properties defined in Table 5.2 with repetition coding factor of 8 had optimum results. Thus, this research work opened a door opened for future research towards PLC in the automotive environment. Furthermore to this, addition of more effective error control coding will make the system more reliable. A feedback enabled communication system setup with high data rate can be another option to provide a more reliable solution for safety critical operations in vehicular implementations. The retransmission of data packets can be included for error control enhancement. Furthermore, the data rate of the system can be increased by increasing the number of active subcarriers and/or by using higher order modulation scheme. Multicarrier CDMA (MC-CDMA) with orthogonal codes, allows to transmit multiple data streams using the same subcarriers, can also result into high data rate PLC in automotive domain.

REFERENCES

[1]   N. Pavlidou, A. J. Han Vinck, J. Yazdani, and B. Honary, "Powerline Communications: state of the Art and Future trends", in *IEEE Communications Magazine*, pp. 34–40, 2003.

[2]   Latchman and Newman, "Homeplug AV Powerline alliance", in *IEEE ISPLC group paper*, 2007.

[3]   Francesco Benzi, Tullio Facchinetti and Thomas Nolte "Towards the Powerline Alternative in Automotive Applications", in *IEEE International Workshop on Factory Communication Systems,* ISBN: 978-1-4244-2350-7/08, 2008.

[4]   E. Arabia, C. Ciofi, A. Consoli, R. Merlino, and A.Testa, "Electromechanical Actuators for Automotive Applications Exploiting Powerline Communication", in *Proc. of the International Symposium on Power Electronics, Electrical Drives, Automation and Motion (SPEEDAM)*, Taormina, Italy, 2006.

[5]   "FlexRay communications system - protocol specification, Version 2.0", in *FlexRay Consortium,* June 2004.

[6]   Miguel Almeida, *Advances in vehicular networking technologies*, India, 2011, InTech.

[7]   Andrea Schiffer, "Statistical Channel and Noise Modeling of Vehicular DC-Lines for Data Communication", in *Vehicular Technology Conference Proceedings, VTC 2000-Spring Tokyo,* vol.1, pp. 158-162, ISBN: 0-7803-5718-3/00, 2000.

[8]   M. Antoniali, M. De Piante and A. M. Tonello, "PLC Noise and Channel Characterization in a Compact Electrical Car", in *Powerline Communications and Its Applications (ISPLC), 17th IEEE International Symposium,* pp. 29-34, ISBN: 978-1-4673-6016-6/13, 2013.

[9]   Prof. Markku Renfors, "Lecture slides on Powerline Communication (PLC)", for *Advanced Course in Digital Transmission* Tampere University of Technology, Fall 2013.

[10]   T. Nolte, H. Hansson, and L. Lo Bello, "Automotive Communications - Past, Current and Future", in *Proceedings of the 10th IEEE International Conference*

on Emerging Technologies and Factory Automation (ETFA), Vol. 1, pp. 985–992, Catania, Italy, September, 2005.

[11]   Y. Maryanka, "Wiring Reduction by Battery Powerline Communication", in *IEEE Seminar on Passenger Car Electrical Architecture*, pp. 8/1-8/4, 2000.

[12]   "HomePlug AV White paper"*,* by *HomePlug® Powerline Alliance, Inc*, Document version number: HPAVWP-050818, 2005.

[13]   Bahai, Saltzberg, and Ergen, M. "Multi Carrier Digital Communications", second edition, ISBN: (HB)0-387-22575-7, Springer, New York, 2004.

[14]   Gavette, S. and al. "HomePlug AV Technology Overview"*,* in *Technical report,* Sharp Laboratories of America*,* 2006.

[15]   Galli, S.; Koga, H. and Kodama, N. "Advance signal processing for PLCs: Wavelet OFDM"*,* in *Proceedings of Powerline Communications and Its Applications,* pp. 187-192, ISBN: 978-1-4244-1975-3, Jeju city, Jeju Island, 2-4 April 2008.

[16]   Benzi, T. Facchinetti, T. Nolte and Almeida L. "Towards the powerline alternative in automotive applications"*,* in *Proceedings of Factory Communication Systems,* pp. 259-262, ISBN: 978-1-4244-2349-1, Dresden, 21-23 May 2008.

[17]   Degardin, V. Laly, P. Liénard, M. and P. Degauque, "Impulsive Noise on In-Vehicle Powerlines: Characterization and Impact on Communication Performance", in *Proceedings of IEEE International Powerline Communications and Its Applications*, pp.222-226, ISBN:1-4244-0113-5, Orlando, 26-29 March 2006.

[18]   Mohammadi, M. Lampe L. Lok, M.; Mirabbasi, S. Mirvakili, M. Rosales, R. and Van Veen, P. "Measurement study and transmission for in-vehicle powerline communication", in *Proceedings of IEEE Powerline Communications and Its Applications*, pp. 73–78, 978-1-4244-3790-0, Dresden, 29-March -1 April 2009.

[19]   De Caro S. and Testa, A. "A Powerline Communication Approach for Body Electronics Modules*,* in *Proceeding of Power Electronics and Applications,* pp. 1-10, 978-1-4244-4432-8, Barcelona, 8-10 September 2009.

[20]   F. Benzi, Tullio Facchinetti and D. Caprini, "Powerline Protocols, Review, Evaluations and Test for Automotive Application", in *International Meeting on Powerline Communication for but not limited to Automotive,* pp 25-30, Tuesday, 4 November 2008.

[21] Silva, P. Almeida, L. Caprini, D. Facchinetti, T. Benzi, F. and Nolte, T. "Experiments on Timing Aspects of DC-Powerline Communications", in *Proceedings of IEEE international Conference on Emerging Technologies and Factory Automation*, pp. 1674-1677, 2009.

[22] Beikirch, H. and Voss, M. "CAN-Transceiver for Field Bus Powerline Communication", in *Proceedings of the International Symposium on Powerline Communications and Its Applications*, Limerick, pp. 257–264, April 2000.

[23] Bassi, E. Benzi, F. Almeida, L. and Nolte, T, "Powerline Communication in Electric vehicles", in *Electric Machines and Drives Conference,* pp. 1749–1753, ISBN: 978-1-4244-4251-5, Miami, 3-6 May 2009.

[24] Barmada, S. Raugi, M. Tucchi, M. and Zheng, T., "Powerline Communication in a Full Electric Vehicle", in *Proceedings of IEEE International Symposium on Powerline Communications and Its Applications*, pp. 331-336, 978-1-4244-5009-1, Rio de Janeiro, 28-31 March 2010.

[25] Nouvel, F. and Maziéro, P. "X-by-Wire and Intra-car Communications: Powerline and/or Wireless Solutions", in *Proceedings of International Conference on Intelligent Transport Systems Telecommunications*, pp. 443-448, 978-1-4244-2857-1, Phuket, 24 October 2008.

[26] J. Bingham, "Multicarrier Modulation for Data Transmission: An Idea Whose Time Has Come", in *IEEE Communications Magazine*, vol. 28 of 5, pp. 5-14, May 1990.

[27] M. Pun, M. Morelli, and C. Kuo, "Multi-Carrier Techniques For Broadband Wireless Communications: A Signal Processing Perspectives", Vol. 3, pp. 17-48, Imperial College Press, 2007.

[28] R. Nee and R. Prasad, "OFDM Wireless Multimedia Communications", Artech House Boston London, 2000.

[29] Y. Shmaliy, Continuous-Time Signals, pp. 14-34, Springer, Netherland, 2006.

[30] S. Mitra, Digital Signal Processing: A Computer-based Approach, fourth edition, McGraw-Hill, 2010.

[31] S. H. Han and J. H. Lee, "An overview of peak-to-average power ratio reduction techniques for multicarrier transmission", in *Wireless Communications, IEEE, vol. 12*, pp. 56-65, 2005.

[32] J. Proakis, Communication systems engineering, second edition, Prentice Hall PTR, 2002, 801 p.

[33] P. Stoica and R. Moses, Spectral analysis of signals, Pearson Prentice Hall, 2005.

[34] T. van Waterschoot, V. Le Nir, J. Duplicy, and M. Moonen, "Analytical Expressions for the Power Spectral Density of CP-OFDM and ZP-OFDM Signals", in *Signal Processing Letters, IEEE*, vol. 17, no. 4, pp. 371-374, 2010.

[35] A. Y. M. Loulou, "Enhanced OFDM for Fragmented Spectrum Use", *Dissertation* 2013, Tampere University of Technology, Dept. of Communication Engineering, pp. 43-47.

[36] J. Armstrong, P. M. Grant, and G. Povey, "Polynomial Cancellation Coding of OFDM to Reduce Inter Carrier Interference due to Doppler Spread", in *Proc IEEE Global Telecommunications Conference*, pp. 2771-2776, Nov. 1998.

[37] K. Panta and J. Armstrong, "Spectral analysis of OFDM signals and its improvement by polynomial cancellation coding", in *Consumer Electronics, IEEE Transactions*, vol. 49, no. 4, pp. 939-943, 2003.

[38] T. Weiss, J. Hillenbrand, A. Krohn, and F. Jondral, "Mutual interference in OFDM-based spectrum pooling systems", in *Proc. IEEE Vehicular Technology Conference (VTC 2004-Spring)*, pp. 1873-1877, May 2004.

[39] A. Sahin and H. Arslan, "The Impact of Scheduling on Edge Windowing", in *Proc. Global Telecommunications Conference*, pp. 1-5 Dec. 2011.

[40] S. Brandes, I. Cosovic, and M. Schnell, "Sidelobe Suppression in OFDM Systems by Insertion of Cancellation Carriers, in *Proc. IEEE Vehicular Technology Conference (VTC-2005-Fall)*, pp. 152-156, Sep. 2005.

[41] I. Cosovic, S. Brandes, and M. Schnell, "Subcarrier Weighting: A Method for Sidelobe Suppression in OFDM Systems", in *Communications Letters, IEEE,* vol. 10, no. 6, pp. 444 to 446, 2006.

[42] Meng-Han Hsieh and Che-Ho Wei, "Channel Estimation for OFDM Systems Based on Comb-Type Pilot Arrangement in Frequency Selective Fading Channels", in *IEEE Transactions on Consumer Electronics,* Vol.44, No.1, Page(s):217 – 225, February 1998.

[43] Professor Markku Renfors, Lecture slides, *ELT-43306 Advanced Course in Digital Transmission,* Tampere University of Technology, Fall 2013.